***Graphical Abstract (for review)**

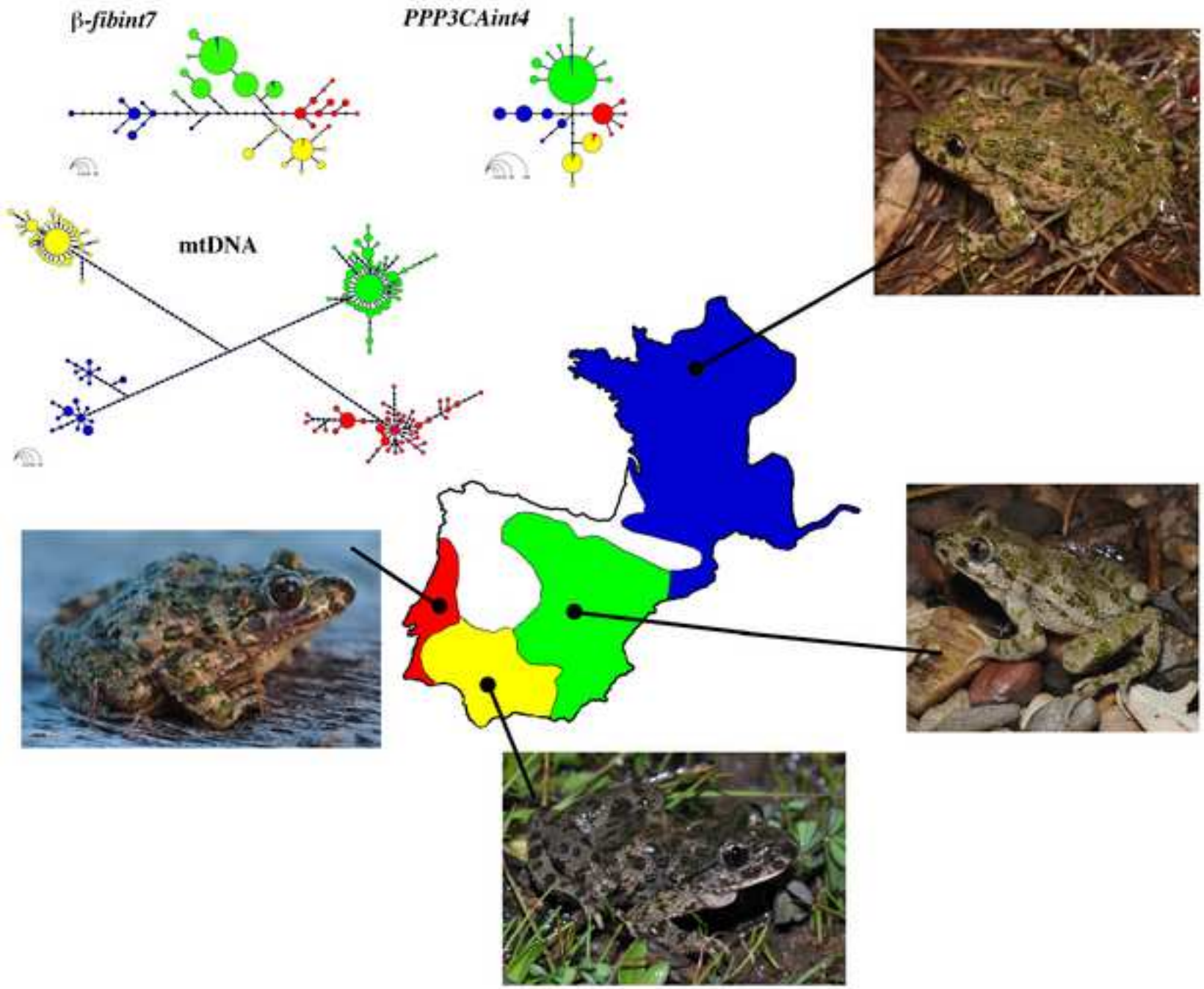

Highlights

Phylogenetic analyses of DNA sequences recover four clades in Iberian Pelodytes frogs

Strong geographic structure and contrasting demographic histories

Well-resolved species trees with Plio-Pleistocene divergence between clades

Information theory validation approach suggests need for taxonomic revision

Species diversity probably underestimated, with two candidate species

Molecular evidence for cryptic candidate species in Iberian *Pelodytes* (Anura, Pelodytidae)

Jesús Díaz-Rodríguez[a,b], Helena Gonçalves[a], Fernando Sequeira[a], Tiago Sousa-Neves[a], Miguel Tejedo[b], Nuno Ferrand[a,c], Iñigo Martínez-Solano[a,d,e,*]

[a] CIBIO-InBIO, Centro de Investigação em Biodiversidade e Recursos Genéticos, Campus Agrário de Vairão, Universidade do Porto, 4485-661 Vairão, Portugal

[b] Department of Evolutionary Ecology, Estación Biológica de Doñana (EBD-CSIC), Avenida Américo Vespucio, s/n, 41092 Sevilla, Spain

[c] Departamento de Zoologia e Antropologia – Faculdade de Ciências da Universidade do Porto, 4099-002 Porto, Portugal

[d] Instituto de Investigación en Recursos Cinegéticos (CSIC-UCLM-JCCM). Ronda de Toledo, s/n, 13005 Ciudad Real, Spain

[e] Ecology, Evolution and Development Group, Department of Wetland Ecology, Estación Biológica de Doñana (EBD-CSIC), Avenida Américo Vespucio, s/n, 41092 Sevilla, Spain

[*] Corresponding author: E-mail: inigomsolano@gmail.com. Present address: Department of Wetland Ecology, Estación Biológica de Doñana (EBD-CSIC), Avenida Américo Vespucio, s/n, 41092 Sevilla, Spain. Phone: +34 954 232 340 ext. 1028; Fax: +34 954 621 125.

Abstract

Species delineation is a central topic in evolutionary biology, with current efforts focused on developing efficient analytical tools to extract the most information from molecular data and provide objective and repeatable results. In this paper we use a multilocus dataset (mtDNA and two nuclear markers) in a geographically comprehensive population sample across Iberia and Western Europe to delineate candidate species in a morphologically cryptic species group, Parsley frogs (genus *Pelodytes*). *Pelodytes* is the sole extant representative of an ancient, historically widely distributed anuran clade that currently includes three species: *P. caucasicus* in the Caucasus; *P. punctatus* in Western Europe, from Portugal to North-Western Italy; and *P. ibericus* in Southern Iberia. Phylogenetic analyses recovered four major well-supported haplotype clades in Western Europe, corresponding to well demarcated geographical subdivisions and exhibiting contrasting demographic histories. Splitting times date back to the Plio-Pleistocene and are very close in time. Species-tree analyses recovered one of these species lineages, corresponding to *P. ibericus* (lineage B), as the sister taxon to the other three major species lineages, distributed respectively in: western Iberian Peninsula, along the Atlantic coast and part of central Portugal (lineage A); Central and Eastern Spain (lineage C); and North-eastern Spain, France and North-western Italy (lineage D). The latter is in turn subdivided into two sub-clades, one in SE France and NW Italy and the other one from NE Spain to NW France, suggesting the existence of a Mediterranean-Atlantic corridor along the Garonne river. An information theory-based validation approach implemented in SpedeSTEM supports an arrangement of four candidate species, suggesting the need for a taxonomic revision of Western European *Pelodytes*.

Keywords: Species delineation, Species trees, Systematics, Amphibians, Iberian Peninsula, *Pelodytes*

1. Introduction

Species delineation, or the grouping of individuals and populations into discrete lineages based on different sets of data and operational criteria, remains one of the central topics in evolutionary biology (Wiens, 2007; Fujita et al., 2012). With the recent and rapid progress of DNA sequencing technologies, the field has quickly shifted focus from issues related to quantity and quality of data (e.g., identification of diagnostic characters, assessment of congruence across datasets) towards the development of more efficient analytical tools. This implies extracting the most information from molecular data, integrating it with morphological, biogeographic and ecological information, thus providing objective, repeatable and robust results in the form of well demarcated, independently evolving lineages that are considered candidate species amenable to further hypothesis testing (Leaché et al., 2009; Rivera et al., 2011; Camargo et al., 2012; Ahrens et al., 2013; Carstens et al., 2013; Edwards and Knowles, 2014). New developments in the field are related to widespread acceptance of de Queiroz's definition of species as "separately evolving metapopulation lineages" (de Queiroz, 2007) and the conceptual shift from gene-tree to species-tree inference, which has transformed the field of molecular systematics (Edwards et al., 2007; Edwards, 2009).

Some of the most challenging systems for delineation of evolutionarily independent lineages include relatively young, morphologically cryptic species groups, where lack of diagnostic characters and conflict between datasets complicates attempts to delineate lineages and infer species trees (Bickford et al., 2007; Weisrock et al., 2010; Florio et al., 2012; Puillandre et al., 2012; Barley et al., 2013). While examples are widespread across many taxonomic groups, amphibians are particularly well represented because, in general, they are morphologically similar, and high historical effective population sizes and/or incomplete reproductive isolation often yield conflicting gene trees (Vences and Wake, 2007; Fontenot et al., 2011; Sequeira et al., 2011; Martínez-Solano et al., 2012; Fouquet et al., 2013; Barrow et al., 2014). The widespread use of molecular markers since the 90's uncovered high levels of "cryptic" amphibian diversity, especially in the tropics (e.g.,

Fouquet et al., 2007; Funk et al., 2012), but also in the more extensively studied temperate regions, notably in areas that acted as glacial refugia during the Pleistocene, like the Iberian Peninsula (Hewitt, 2004; Weiss and Ferrand, 2007; Recuero et al., 2012; Stöck et al., 2012).

An interesting case study is represented by Eurasian Parsley frogs (genus *Pelodytes*), including three extant species, one in the Caucasus (*P. caucasicus*), and two in Western Europe: *P. punctatus,* distributed throughout most of the Iberian Peninsula and also present in France and coastal northwestern Italy (Denöel et al., 2013), and the Iberian endemic *P. ibericus* (Barbadillo, 2002). According to the fossil record, *Pelodytes* has a long history in Western Europe, where it was widely distributed (see review in Martín and Sanchiz, 2014), including fossil taxa (*Pelodytes arevacus*) dating back to the Miocene (9.7-22.5 million years –myr- ago, Sanchiz, 1978, 1998; Martín and Sanchiz, 2014) and closely resembling extant Iberian species in osteological characters (Sanchiz et al., 2002). Fossils morphologically ascribed to *P. punctatus* that are at least 3.2 myr old have been reported in southeastern France (Blain, 2009). Therefore, and taking into account the role of the Iberian Peninsula as a hotspot for inter- and intraspecific differentiation across a large number of taxa (Abellán and Svenning, 2014), additional opportunities for speciation in Iberian *Pelodytes* may have existed, and current species diversity may be underestimated. In fact, a recent study suggested the existence of additional, cryptic species in southwestern Iberia (van de Vliet et al., 2012).

In the present study we use DNA sequences from a comprehensive sample of 384 individuals from 160 Iberian populations to delineate major independently evolving lineages in *Pelodytes* through a combination of discovery and validation species-delineation approaches. Our results indicate the existence of additional candidate species in the genus, help to identify their contact zones and provide new insights into the timing and geography of their diversification.

2. Material and methods

2.1 Sampling and DNA extraction

We sampled one to 12 individuals per population in a total of 160 localities spread across the extant ranges of *P. punctatus* and *P. ibericus*, including seven individuals of *P. caucasicus* that were used as outgroup (Fig. 1, Table 1). A total of 391 individuals (including the outgroup) were used for subsequent molecular analyses (Table 1). Tissue samples were obtained from either tail tips of larvae and/or toe tips of adults and preserved in 70% ethanol or frozen. Whole genomic DNA was extracted using the commercial DNA extraction kit Dneasy® Tissue Kit (Qiagen, Hilden, Germany) following the manufacturers' instructions or with the standard high-salt protocol of Sambrook et al. (1989).

2.2 Molecular markers, amplification and sequencing

Four markers, including two mitochondrial (mtDNA) and two nuclear (nDNA) gene fragments were analyzed: 705 bp of cytochrome b (*cob*), 788 bp of NADH dehydrogenase subunit 4 (*nad4*) (including adjacent tRNAs), a fragment of 393 bp of protein phosphatase 3 catalytic subunit alpha isoform intron 4 (*PPP3CAint4*), and 752 bp of beta fibrinogen intron 7 (*β-fibint7*). All markers were amplified via the polymerase chain reaction (PCR) using the following combination of primers and PCR thermal cycling conditions. For *cob*, reactions were performed with primers "L14724" (Irwin et al., 1991), and "MVZ16" (Moritz et al., 1992) with initial denaturation at 94 ºC for 3 min; 35 cycles with a denaturing temperature of 92 ºC (40 s), annealing at 47 ºC (1 min), and extension at 72 ºC (1 min and 20 s) followed by final extension at 72 ºC for 5 min. For *nad4* we used primers ND4 and Leu, previously described by Arevalo et al. (1994), with an initial denaturation at 94 °C (5 min); followed by 35 cycles of denaturation at 94 °C (40 s), annealing at 56 °C (1 min), extension at 72 °C (1 min and 20 s); and final extension of 72 °C for 5 min. Additionally, sequences of *PPP3CAint4* were amplified with PCR conditions described by Pinho et al. (2010), consisting of an initial denaturation at 94 ºC for 3 min; 40 cycles with a denaturing temperature of 94 ºC (30 s), annealing at 53 ºC (1min), and extension at 72 ºC (1 min and 30 s), with a final extension at 72 ºC for 5 min. Amplified fragments were sequenced in both directions.

For *β-fibint7* a two-step amplification procedure was used, with a combination of two primer pairs (PCR1: FIBX7 and FIBX8; PCR2: BFXF and BFXR) as described by Sequeira et al. (2006), with an initial denaturation at 94 °C for 3 min, followed by 40 cycles of denaturing at 94 °C (40 s), annealing at 50 °C (PCR1) and 56 °C (PCR2), (1 min), extension at 72 °C (1min 30 s) and a final extension of 72 °C for 5 min. Amplified fragments of PCR2 were also sequenced in both directions using the primers BFXF and BFXR. In both nuclear markers, indels present only in the outgroup and regions in the alignment that could not be unambiguously edited or aligned due to the presence of short repeats were excluded prior to further analyses (reported alignment sizes take into account exclusion of these sites).

PCRs were performed in a total volume of 10 µl, including 0.1 µl Taq polymerase (5 U/µl Biotaq® and Bioline DNA Polymerase); 0.1 µl BSA (20 mg/ml); 0.5 µl of each primer (5 µM); 0.1 µl dNTPs (25 mM); and 0.3 µl of $MgCl_2$ (50 mM) plus 1 µl of reaction Buffer. For *PPP3CAint4*, PCRs were performed in a total volume of 10 µl, including 0.1 µl of EcoTaq polymerase (5 U/µl Taq DNA Polymerase, EcoGen); 0.3 µl of each primer (10 µM); 0.5 µl dNTPs (40 µM); and 0.5 µl of $MgCl_2$ (50 mM) plus 1 µl of reaction Buffer NH3 (Bioline).

After PCR products were purified with Montage PCR columns (Millipore), samples were cycle-sequenced using ABI Prism Big Dye Terminator Cycle in an ABI PRISM® 310 automated sequencer (Applied Biosystems) following the manufacturers' instructions.

2.3. Lineage identification and delineation

Sequences were checked by eye, edited and aligned using the program Bioedit v7.2.5 (Hall, 1999). All sequences generated for this study are deposited in GenBank under Accession Nos. KP165846-KP167135 (Table 1). Polymorphic positions corresponding to heterozygous individuals in nuclear loci were coded with IUPAC ambiguity codes. Haplotypes were phased using PHASE v2.1 (Stephens et al., 2001; Stephens and Donnelly, 2003), using SeqPHASE (Flot, 2010) to format the input files. Length variant heterozygotes (LVHs), which resulted from the amplification of

alleles with different sizes from a single individual, were phased interpreting directly the mixed trace in the electropherogram formed by the two allelic peaks superimposed onto each other downstream of the indel (e.g. Sousa-Neves et al., 2013). All known haplotypes were incorporated for subsequent haplotype inference. We accepted haplotypes with a minimum probability of 0.9.

We performed phylogenetic analyses in MrBAYES v3.2.1 (Huelsenbeck and Ronquist, 2001; Ronquist et al., 2012) to estimate relationships between mtDNA and nDNA haplotypes. Full alignments were collapsed into haplotypes using the online tool Fabox (Villesen, 2007). For the mtDNA dataset, we used PartitionFinder v1.1.1 (Lanfear et al., 2012) to choose the optimal partitioning strategy. Best support was obtained for three partitions, corresponding to first positions in *cob* and *nad4* and the fragment containing the tRNAs; second positions in *cob* and *nad4*; and third positions in *cob* and *nad4*. Analyses in MrBAYES were set to explore the full GTR parameter space in each of the three partitions using the commands nst=mixed rates=invgamma. Convergence of results was assessed by examination of values of the standard deviation of split frequencies across runs and visual inspection of parameter values during the run in Tracer v1.6 (Rambaut et al., 2014).

Genealogical relationships among haplotypes for each locus were estimated using phylogenetic algorithms as implemented in Haploviewer (Salzburger et al., 2011). Phylogenetic relationships among haplotypes for each locus were estimated using a Maximum Likelihood (ML) approach, as implemented in the software RAxML v7.0.4 (Silvestro & Michalak, 2010), using the graphical front-end RAxML GUI v0.93 (Randomized Accelerated Maximum Likelihood; Stamatakis, 2006). Using default options we ran the program with the best fit model for each locus as selected by PartitionFinder v0.9 (Lanfear et al., 2012) under the Akaike information criterion (AIC; Akaike, 1973), and the generated trees were used to estimate each haplotype network.

We assessed probability of recombination in nuclear sequences with TOPALi v2.5 (Milne et al., 2004), using the difference of sums of squares (DSS) method with a sliding window of 100-bp

and 10-bp step size, and also with the PhiTest implemented in Splitstree v4.2 (Huson and Bryant, 2006).

Four major lineages of Iberian *Pelodytes* were recovered in previous analyses (see results below) and for each of them several genetic diversity parameters were estimated. In addition, we performed a pairwise mismatch distribution analysis (Rogers and Harpending, 1992), and calculated several statistics including Tajima's D (Tajima, 1989), Ramos-Onsins and Rozas' R^2 (Ramos-Onsins and Rozas, 2002) and Fu's Fs (Fu, 1997) to test for signatures of demographic expansion in each of the four lineages using DnaSP v5.10 (Librado and Rozas, 2009). Genetic distances (p-uncorrected) within and between species lineages were calculated with Mega v6 (Tamura et al., 2013).

Species trees were reconstructed based on two different methodologies. First, we used the coalescent-based method implemented in *BEAST (Heled and Drummond, 2010). We used a Yule speciation prior with strict molecular clock. Each marker was analyzed as an independent partition, with nucleotide substitution models selected by jModeltest v2.1.1, based on the Bayesian Information Criterion (Darriba et al., 2012). Tree topologies and molecular clocks across partitions were unlinked. We specified a lognormal prior for the substitution rate of the mtDNA partition with a mean of 0.0075 substitutions/site/myr and a standard deviation of 0.2, encompassing values typically reported in the literature (see for example Recuero et al., 2012). Three independent analyses were run for one hundred million generations and trees and other parameters were sampled every 10,000 generations. Traces were visualized in Tracer v1.6 (Rambaut et al., 2014) to check for adequate mixing and convergence of results across runs, and log and treefiles were subsequently combined. Additionally, we used the pseudo-likelihood approach implemented in MP-EST v1.3 (Liu et al., 2010) to infer the *Pelodytes* species tree. To estimate branch support, 1,000 replicate gene trees for each marker (taken from the post burn-in sample of trees from a MrBAYES run, see above) were subjected to MP-EST analyses to derive bootstrap proportions of inferred clades in the species tree. MP-EST analyses were run in the STRAW server (Shaw et al., 2013). Both *BEAST

and MP-EST attribute gene-tree discordance to incomplete lineage sorting and do not take into account gene flow across population lineages; therefore, individuals and populations identified as admixed based on inspection of the mtDNA tree and nDNA haplotype networks (see results below) were excluded from the datasets prior to analyses. All other individuals from populations where mtDNA haplotypes from different lineages were found in sympatry were also excluded.

2.4. Validation approach

We used SpedeSTEM (Ence and Carstens, 2011) as a validation approach to evaluate support for the previously identified candidate species. SpedeSTEM calculates the likelihood of multiple arrangements of putative evolutionary lineages based on externally generated gene trees and ranks them by model probability using information theory. Gene trees were estimated by maximum-likelihood inference in Garli v0.951 (Zwickl, 2006) using alignments with a single representative per haplotype (excluding admixed populations, as in previous analyses). We used a weighted average across loci calculated in DnaSP as the estimate for theta (theta= 0.03093), with a scaling (variable sites/total sites) of 1:0.47:0.32 for mtDNA, *β-fibint7* and *PPP3CAint4*, respectively. *Pelodytes caucasicus* was used as outgroup, with the remaining samples divided into two major groups corresponding to *P. ibericus* and *P. punctatus*, with the latter subdivided into the three lineages recovered in previous analyses. Analyses were run online in the SpedeSTEM server at: https://spedestem.osu.edu/runspedestem.

3. Results

Amplification of the two mtDNA fragments was successful in 367 individuals (including seven outgroup samples, Table 1), yielding an alignment of 1493 bp with 155 unique haplotypes (375 variable sites, 321 parsimony-informative). Additionally, 139 individuals (278 phased sequences) from the ingroup plus two from the outgroup were sequenced for *PPP3CAint4* (393 bp) and *β-fibint7* (752 bp). Different individuals were sequenced for each nuclear marker (see Table 1). An A+T-biased content was observed in *PPP3CAint4* sequences, which is consistent with values

reported for this marker in other species (according to Prychitko and More, 1997, this feature of A-T rich sequences is a peculiarity of non-coding regions that are not under functional constraint). There were 23 unique haplotypes in *PPP3CAint4* (25 variable sites, 13 parsimony-informative); and 40 haplotypes in *β-fibint7* (45 polymorphic sites, 31 parsimony-informative). Table 1 lists individuals sequenced for each marker. We did not find significant evidence of recombination in the nuclear markers.

Phylogenetic analyses of mtDNA data recovered a well-resolved tree with four major haplotype clades (labeled A to D), with a strong association with geography (Figs. 1 and 2). Clade B corresponds to *P. ibericus*, whereas the remaining clades (A, C and D) are ascribed to *P. punctatus*: A is distributed in the south-west of the Iberian Peninsula, along the Atlantic coast and part of central Portugal; C occupies central and eastern Spain; and D is present in north-eastern Spain, France and north-western Italy. All four major clades are well supported by Bayesian Posterior Probabilities (BPP) of 0.99-1.0. Clade D is subdivided in two well-supported sub-clades, one containing samples from NW Italy and SE France (localities 152 to 157, BPP: 1.0) and the other with the remainder of samples (BPP: 0.99). Clades A, C and D form a monophyletic group (BPP: 0.96), with D being the sister taxon to (A+C), although with moderate support (BPP: 0.86). In some populations, we found haplotypes of different clades co-occurring (Table 1 and Fig. 1). These include localities 17-21 (clades A + B), and 75, 88 (clades B+C). We found no localities with mtDNA haplotypes of clades C+D occurring in sympatry.

Estimates of genetic diversity and intra- and interpopulation genetic distance are shown in Tables 2 and 3, respectively. For mtDNA, we found moderate levels of genetic diversity in haplotype clades B and C, with higher values of haplotype and nucleotide diversity in clades A and D. Mismatch distribution plots revealed a clearly unimodal pattern in clades A, B and C, suggesting demographic expansion (Fig. S1). This is in accordance with significant values of Tajima's D, Fu's Fs and Ramos-Onsins & Rozas' R^2 statistics in the same clades (Table 2). In contrast, clade D exhibits a multimodal mismatch distribution, with no significant values for any statistic, suggesting

demographic stability or genetic substructuring. The average number of pairwise sequence differences (p-uncorrected distance) between clades ranged from 3.3% to 4.4% (Table 3), whereas between each of the Iberian clades and *P. caucasicus* the values ranged from 15.7-16.8%. Within clades, p-distances were higher in clade D (0.64%) than in the other clades (0.12-0.37%, Table 3). We interpret haplotype clades A-D to diagnose four species lineages.

Haplotype networks based on mtDNA and nuclear sequences are shown in Fig. 3. In mtDNA, lineages B and C exhibit star-like topologies, with one high frequency, central haplotype and several additional haplotypes connected by one-step mutations, again suggesting recent demographic expansion. The most frequent haplotype in lineage B was present in 42 out of 94 sequences and was widely distributed, with 23 haplotypes occurring only once and 10 additional haplotypes with frequencies 2-9. The most frequent haplotype in lineage C occurred in 50 out of 151 individuals from the center and east of the Iberian Peninsula, with 37 haplotypes with a frequency of 1 and an additional 17 haplotypes with frequencies 2-9. Lineage A was subdivided into two main haplotype groups, one of them largely distributed in central (Setúbal, Lisboa and Santarém) and Northern Portugal (Porto and Coimbra), and the other geographically restricted to the south (Faro). We found 42 haplotypes in this lineage, with a highest frequency of 15 and 30 haplotypes observed only once. Finally, lineage D includes two major haplotype groups: a) from Catalonia to Northwestern France; and b) from Southern France (Provence-Côte D'Azur) to Northern Italy (Liguria). We found a total of 20 haplotypes in this lineage, with frequencies ranging from 1-6. Nuclear networks were congruent with mtDNA, with four major haplotype groups in each marker (Fig. 3), but we also detected the presence of heterozygous individuals with alleles clustering with different lineages, especially in areas of close geographic proximity between them (lineages A+B: populations 17, 18, 21; lineages B+C: population 88; lineages C+D: population 143, see Table 1 and Fig. 1). Some individuals had mtDNA haplotypes characteristic of one lineage and nuclear alleles of a different lineage (lineages C+D, populations 143, 144, 150, Table 1, Fig. 1).

283 Species tree analyses recovered concordant, robust topologies, with *P. ibericus* (lineage B)
284 being the sister taxon to a clade including the other three major linages (BPP: 0.89, bootstrap
285 support -Bs-: 100), with lineage D being the sister taxon to (A+C) (BPP: 0.75; Bs: 87.6). According
286 to *BEAST results, major speciation events in Iberia occurred in the Pliocene and Lower
287 Pleistocene (Fig. 4). Median and 95% highest posterior density intervals (HPDs) for inferred splits
288 were 3.63 (2.07-5.50) myr (*P. ibericus vs.* lineages A, C and D; 2.91 (1.68-4.51) myr for lineage D
289 *vs.* lineages A+C; and 2.86 (1.54-4.48) myr for lineages A and C (Fig. 4).
290 The SpedeSTEM-based validation approach provided the highest support for the four-
291 lineage arrangement (Table 4), supporting their qualification as candidate species (*P. ibericus* plus
292 three candidate species, one of which would retain the name *P. punctatus*, see Discussion).
293
294 **4. Discussion**
295 Initial attempts at probabilistic, molecular-based species delineation were received with
296 criticism (Bauer et al., 2011; Fujita and Leaché, 2011), but in a short time these methods have
297 become more popular. However, they have not replaced character-based species descriptions, and
298 thus the lineages identified in species delineation analyses are best treated as candidate species, or
299 species hypotheses amenable to further testing with as many different sources of evidence as
300 possible. Our approach, based on multilocus analyses of a comprehensive sample, consistently
301 recovered four historical lineages in Iberian *Pelodytes*, showing strong geographic structuring
302 (lineages A-D, Figs. 1-4). Of these, one corresponds to *Pelodytes ibericus* (lineage B), which has
303 been shown to differ in morphological, osteological, behavioral (mating calls), and molecular
304 characters from populations ascribed to *P. punctatus* (Sánchez-Herráiz et al., 2000; Sanchiz et al.,
305 2002; Pargana et al., 2003; García-París et al., 2003; Veith et al., 2006). In our analyses, *P. ibericus*
306 is also recovered as diverging from the rest of the Iberian lineages around 3.6 myr ago, in
307 accordance with previous estimates based on allozymes and mtDNA data (3.3-3.8 myr, see
308 Sánchez-Herráiz et al., 2000; Sanchiz et al., 2002; García-París et al., 2003). Contact zones with

lineages A and C have been approximately identified (Fig. 1), and further fine-scale sampling coupled with detailed analysis using a large set of fast-evolving nuclear markers (microsatellites or single nucleotide polymorphisms) will be of crucial importance to assess the extent of reproductive isolation across lineages (which is incomplete, as shown by our observation of several instances of cyto-nuclear discordance; see also van de Vliet et al., 2012, where boundaries between lineages A and B slightly differ from our results).

The second most differentiated lineage (lineage D) includes all populations north of the Pyrenees, and since it includes the type locality of *P. punctatus* ("aux environs de Beauvais", Department Oise, northern France: Daudin, 1802) it would retain this name. Two sub-clades were strongly supported in phylogenetic analyses of mtDNA sequences. One of these groups includes populations in SE France and NW Italy, whereas the other one is more widely distributed from NE Spain (Catalonia) to northern France. Remarkably, there is little genetic differentiation in this second sub-clade. The pattern of haplotypic diversity, with more haplotypes in populations south of the Pyrenees, suggests a rapid, recent expansion, probably along the Garonne river basin, which provides a corridor connecting the Atlantic and Mediterranean coasts of France. The genetic distinctiveness of these populations had previously been noted by Sánchez-Herráiz et al. (2000) and García-París et al. (2003). Relatively high levels of genetic diversity in lineage D are consistent with a long fossil record, possibly dating back to 3.2 myr ago (Sète, see Blain, 2009). Further research is needed to delineate the contact zone with lineage C, although the finding of instances of cyto-nuclear discordance in populations 143, 144 and 150 suggests a wide area of admixture. Surprisingly, haplotypes of lineages C and D were never found in sympatry, although this may be an artifact of sparser sampling at the potential contact zone.

Lineage A is endemic to Portugal, with populations all along its Atlantic coast. Genetic distinctiveness of populations in this area was initially reported by Pargana (1998), who also noted differences in bioacoustic parameters, and more recently by van de Vliet et al. (2012), who reported strong cross-amplification failure in microsatellite markers developed from samples in SW Portugal

when tested in samples from northern Spain (which would correspond to lineage C in our study, see Fig. 1). The existence of well-differentiated linages in SW Portugal has been previously reported for other amphibian species, like *Salamandra salamandra*, *Lissotriton boscai* or *Alytes cisternasii* (Reis et al., 2011; Martínez-Solano et al., 2006; Gonçalves et al., 2009). The addition of *Pelodytes* to an increasing group of taxa with important genetic reservoirs in this region makes it one of the key Iberian "refugia within refugia" (Gómez & Lunt, 2007; Abellán and Svenning, 2014). The existence of putative Pleistocene glacial refugia in Southern Portugal, Spain and France, on the basis of our data and previous studies with other taxa, has strong implications for regional conservation planning. Understanding cryptic diversity is a concern as amphibian habitat, temporary ponds in traditional Mediterranean farmland, is disappearing at a fast rate (Ferreira and Beja, 2013).

Finally, lineage C is the most widespread in Iberia, with populations in the two major plateaus in central Spain. The presence of *Pelodytes* in the Northern Plateau dates back at least to the Early Pleistocene in Atapuerca (Cuenca-Bescós et al., 2010) and is relatively well documented in other (more recent) sites within the current range of this lineage (for example, see Blain et al., 2007, 2011). In spite of this, levels of genetic diversity are comparatively low in this lineage, and with lineage B (*P. ibericus*), it is the only one where all tests of demographic expansion were significant (Table 2, Fig. S1). The harsher climatic conditions of central Spain may have subjected *Pelodytes* populations to strong demographic fluctuations through time, although it remains unclear what circumstances governed long-term demographic trends in *P. ibericus.* Species distribution models (SDMs) are a powerful tool to identify potential differences across lineages in their ecological niche, which may be important to understanding the speciation process (Fitze et al., 2011). However, a recent approach to examining functional divergence between lineages A, B and C revealed weak differentiation in thermal physiology (M. Katzenberger, J. Díaz-Rodríguez, H. Duarte, J.F. Beltrán and M. Tejedo, unpublished data).

Molecular-based species delimitation approaches are rapidly becoming popular in molecular systematics because they allow rapid and objective identification of major historical lineages as

candidate species. Results of our species-delimitation approach suggest that species diversity in Iberian *Pelodytes* may be currently underestimated, with up to two additional lineages that may warrant recognition as new species. More detailed analyses of contact zones, as well as morphological and ecological comparisons of populations representing all major lineages are underway in order to provide robust evidence supporting (or rejecting) these species hypotheses.

Acknowledgments

We thank the editor and two anonymous reviewers for constructive comments on the manuscript. For technical support during lab work we thank Susana Lopes, C. Pinho, M.J. Fernández Benéitez and Bruno Carvalho. We also thank E. Albert, J.W. Arntzen, E. Ayllón, M. Barbosa, A. Bermejo, M. Berroneau, W. Böhme, G. Caballero, D. Canestrelli, T. Couturier, E.G. Crespo, D. Donaire, L. García Cardenete, M. García París, P. Geniez, I. Gómez Mestre, J.P. González de la Vega, E.G. González, A. Gosá, J. Gutiérrez, P. Hernández Sastre, A. Montori, J.C. Monzó, N. Oromí, B. Paños, P. Pavón, E. Recuero, V. Sancho, I. Urbán, A. Valdeón and M. Veith for sharing samples and/or help during fieldwork. A. Sánchez Vialas kindly provided pictures of individuals of lineages A and D, and Godfried Schreur and Ana Cordero, of lineage B (*P. ibericus*). This work was supported through Project "Genomics and Evolutionary Biology" cofinanced by North Portugal Regional Operational Programme 2007/2013 (ON.2 – O Novo Norte), under the National Strategic Reference Framework (NSRF), through the European Regional Development Fund (ERDF); the Program Operacional Factores de Competitividade (COMPETE), and by national funds from Fundação para a Ciência e a Tecnologia (FCT), through the research Projects PTDC/BIA-BEC/099915/2008 and PTDC/BIA-BEC/105083/2008 to HG and FS, respectively; and grants CGL2008-04271-C02-01/BOS and CGL2011-28300 (Ministerio de Ciencia e Innovación, Ministerio de Economía y Competitividad, Spain, and FEDER) and PPII10-0097- 4200 (Junta de Comunidades de Castilla la Mancha and FEDER) to IMS, who was funded by Project "Biodiversity, Ecology and Global Change", co-financed by North Portugal Regional Operational

Programme 2007/2013 (ON.2–O Novo Norte), under the National Strategic Reference Framework (NSRF), through the European Regional Development Fund (ERDF) and is currently supported by funding from the Spanish Severo Ochoa Program (SEV-2012-0262). Additional funds were provided by grants: "Anfibios Endémicos de Andalucía" (Consejería de Medio Ambiente, Junta de Andalucía, Spain), and CGL2005-02931/BOS (Ministerio de Ciencia e Innovación, Spain) to MT. JDR is supported by a PhD grant from FCT (SFRH/BD/70631/2010), HG and FS are supported by postdoctoral grants from FCT (SFRH/BPD/26555/2006 and SFRH/BPD/87721/2012, respectively) and TSN by a research grant (BI) from ICETA/UP.

References

Abellán, P., Svenning, J.C., 2014. Refugia within refugia–patterns in endemism and genetic divergence are linked to Late Quaternary climate stability in the Iberian Peninsula. Biological Journal of the Linnean Society 113, 13–28.

Ahrens, D., Fabrizi, S., Šipek, P., Lago, P.K., 2013. Integrative analysis of DNA phylogeography and morphology of the European rose chafer (*Cetonia aurata*) to infer species taxonomy and patterns of postglacial colonisation in Europe. Molecular Phylogenetics and Evolution 69, 83–94.

Akaike, H., 1973. Information theory as an extension of the maximum likelihood principle. In: Petrov, B.N., Csaki, F. (Eds.), Second International Symposium of Information Theory. Akademiai Kiado, Budapest, Hungary.

Arévalo, E., Davis, S.K., Sites, J.W., 1994. Mitochondrial DNA sequence divergence and phylogenetic relationships among eight chromosome races of the *Sceloporus grammicus* complex (Phrynosomatidae) in central Mexico. Syst. Biol. 43, 387–418.

Bauer, A.M., Parham, J.F., Brown, R.M., Stuart, B.L., Grismer, L., Papenfuss, T.J., Böhme, W., Savage, J.M., Carranza, S., Grismer, J.L., Wagner, P., Schmitz, A., Ananjeva, N.B., Inger,

412 R.F., 2011. Availability of new Bayesian-delimited gecko names and the importance of
413 character-based species descriptions. Proc. Biol. Sci. 278, 490–492.
414 Barbadillo, L.J., 2002. *Pelodytes ibericus*. In: Atlas de distribución y Libro Rojo de los Anfibios y
415 Reptiles de España. eds. J. M. Pleguezuelos, R. Márquez, and M. Lizana, p. 97-99.
416 Dirección General de Conservación de la Naturaleza-Asociación Herpetológica Española,
417 Madrid.
418 Barley, A.J., White, J., Diesmos, A.C., Brown, R.M., 2013. The challenge of species delimitation at
419 the extremes: diversification without morphological change in Philippine sun skinks.
420 Evolution 67, 3556–3572.
421 Barrow, L.N., Ralicki, H.F., Emme, S.A., Lemmon, E.M., 2014. Species tree estimation of North
422 American chorus frogs (Hylidae: *Pseudacris*) with parallel tagged amplicon sequencing.
423 Molecular Phylogenetics and Evolution 75, 78–90.
424 Bickford, D., Lohman, D., Sodhi, N.S., Ng, P.K.L., Meier, R., Winker, K., Ingram, K., Das, I.,
425 2007. Cryptic species as a window on diversity and conservation. Trends in Ecology &
426 Evolution 22, 148–155.
427 Blain, H.A., 2009. Contribution de la paléoherpétofaune (Amphibia & Squamata) à la connaissance
428 de l´évolution du climat et du paysage du Pliocène supérieur au Pléistocène moyen
429 d´Espagne. Treb. Mus. Geol. Barcelona 16, 39-170.
430 Blain, H., Bailon, S., Agustí, J., 2007. Anurans and squamate reptiles from the latest Early
431 Pleistocene of Almenara-Casablanca-3 (Castellón, East of Spain). Systematic, climatic and
432 environmental considerations. Geodiversitas 29, 269–295.
433 Blain, H.-A., López-García, J.M., Cuenca-Bescós, G., 2011. A very diverse amphibian and reptile
434 assemblage from the late Middle Pleistocene of the Sierra de Atapuerca (Sima del Elefante,
435 Burgos, Northwestern Spain). Geobios 44, 157–172.
436 Camargo, A., Morando, M., Avila, L.J., Sites, J.W., Jr, 2012. Species delimitation with ABC and
437 other coalescent-based methods: a test of accuracy with simulations and an empirical

438 example with lizards of the *Liolaemus darwinii* complex (Squamata: Liolaemidae).
439 Evolution 66, 2834–2849.
440 Carstens, B.C., Pelletier, T.A., Reid, N.M., Satler, J.D., 2013. How to fail at species delimitation.
441 Molecular Ecology 22, 4369–4383.
442 Cuenca-Bescós, G., Rofes, J., López-García, J.M., Blain, H.-A., De Marfá, R., Galindo-Pellicena,
443 M.A., Bennàsar, M., Melero-Rubio, M., Arsuaga, J.L., Bermúdez de Castro, J.M.,
444 Carbonell, E., 2010. Biochronology of Spanish Quaternary small vertebrate faunas.
445 Quaternary International 212, 109–119.
446 Darriba, D., Taboada, G.L., Doallo, R., Posada, D., 2012. jModelTest 2: more models, new
447 heuristics and parallel computing. Nature Methods 9, 772.
448 Daudin, F.-M., 1802 "An. XI". Histoire Naturelle des Rainettes, des Grenouilles et des Crapauds.
449 Quarto version. Paris: Levrault.
450 Denoël, M., Beja, P., Andreone, F., Bosch, J., Miaud, C., Tejedo, M., Lizana, M., Martínez-Solano,
451 I., Salvador, A., García-París, M., Recuero Gil, E., Marquez, R., Cheylan, M., Diaz
452 Paniagua, C., Pérez-Mellado, V., 2009. *Pelodytes punctatus*. In: IUCN 2013. IUCN Red List
453 of Threatened Species. Version 2013.2. <www.iucnredlist.org>. Accessed June 09 2014.
454 de Queiroz, K., 2007. Species concepts and species delimitation. Syst. Biol. 56, 879-886.
455 Edwards, S.V., 2009. Is a new and general theory of molecular systematics emerging? Evolution 63,
456 1–19.
457 Edwards, S.V., Liu, L., Pearl, D.K., 2007. High-resolution species trees without concatenation.
458 Proceedings of the National Academy of Sciences 104, 5936–5941.
459 Edwards, D.L., Knowles, L.L., 2014. Species detection and individual assignment in species
460 delimitation: can integrative data increase efficacy? Proceedings of the Royal Society B:
461 Biological Sciences 281, 20132765.
462 Ence, D.D., Carstens, B.C., 2011. SpedeSTEM: a rapid and accurate method for species
463 delimitation. Molecular Ecology Resources 11, 473–480.

464 Ferreira, M., Beja, P., 2013. Mediterranean amphibians and the loss of temporary ponds: are there
465 alternative breeding habitats? Biological Conservation 165, 179–186.
466 Fitze, P.S., Gonzalez-Jimena, V., San-Jose, L.M., San Mauro, D., Aragon, P., Suarez, T., Zardoya,
467 R., 2011. Integrative analyses of speciation and divergence in *Psammodromus hispanicus*
468 (Squamata: Lacertidae). BMC Evol Biol 11, 347.
469 Florio, A.M., Ingram, C.M., Rakotondravony, H.A., Louis, E.E., Raxworthy, C.J., 2012. Detecting
470 cryptic speciation in the widespread and morphologically conservative carpet chameleon
471 (*Furcifer lateralis*) of Madagascar. Journal of Evolutionary Biology 25, 1399-1414.
472 Flot, J.-F., 2010. SeqPHASE: a web tool for interconverting PHASE input/output files and FASTA
473 sequence alignments. Mol. Ecol. Resour. 10, 162–166.
474 Fontenot, B.E., Makowsky, R., Chippindale, P.T., 2011. Nuclear-mitochondrial discordance and
475 gene flow in a recent radiation of toads. Molecular Phylogenetics and Evolution 59, 66–80.
476 Fouquet, A., Gilles, A., Vences, M., Marty, C., Blanc, M., Gemmell, N.J., 2007. Underestimation of
477 species richness in neotropical frogs revealed by mtDNA analyses. PLoS ONE 2, e1109.
478 Fouquet, A., Santana Cassini, C., Fernando Baptista Haddad, C., Pech, N., Trefaut Rodrigues, M.,
479 2013. Species delimitation, patterns of diversification and historical biogeography of the
480 Neotropical frog genus *Adenomera* (Anura, Leptodactylidae). Journal of Biogeography 41,
481 855–870.
482 Fu, Y.X., 1997. Statistical tests of neutrality of mutations against population growth, hitchhiking
483 and background selection. Genetics 147, 915- 925
484 Fujita, M.K., Leaché, A.D., 2011. A coalescent perspective on delimiting and naming species: a
485 reply to Bauer et al. Proc. Biol. Sci. 278, 493–495.
486 Fujita, M.K., Leaché, A.D., Burbrink, F.T., McGuire, J.A., Moritz, C., 2012. Coalescent-based
487 species delimitation in an integrative taxonomy. Trends in Ecology & Evolution 27, 480–
488 488.

489 Funk, W.C., Caminer, M., Ron, S.R., 2012. High levels of cryptic species diversity uncovered in
490 Amazonian frogs. Proceedings of the Royal Society B: Biological Sciences 279, 1806–1814.
491 García-París, M., Buchholz, D., Parra-Olea, G., 2003. Phylogenetic relationships of Pelobatoidea
492 re-examined using mtDNA. Molecular Phylogenetics and Evolution 28, 12–23.
493 Gómez, A., Lunt, D., 2007. Refugia within refugia: patterns of phylogeographic concordance in the
494 Iberian Peninsula. Phylogeography in Southern European Refugia: Evolutionary
495 Perspectives on the Origins and Conservation of European Biodiversity 155–188.
496 Gonçalves, H., Martínez-Solano, I., Pereira, R.J., Carvalho, B.M., García-París, M., Ferrand, N.,
497 2009. High levels of population subdivision in a morphologically conserved Mediterranean
498 toad (*Alytes cisternasii*) result from recent, multiple refugia: evidence from mtDNA,
499 microsatellites and nuclear genealogies. Molecular Ecology 18, 5143–5160.
500 Hall, T.A., 1999. BioEdit: a user-friendly biological sequence alignment editor and analysis
501 program for Windows 95/98/NT. Nucl. Acids. Symp. Ser. 41, 95-98.
502 Heled, J., Drummond, A.J., 2010. Bayesian inference of species trees from multilocus data. Mol.
503 Biol. Evol. 27, 570–580.
504 Hewitt, G.M., 2004. Genetic consequences of climatic oscillations in the Quaternary. Philosophical
505 Transactions of the Royal Society of London. Series B: Biological Sciences 359, 183-195.
506 Huelsenbeck, J.P., Ronquist, F., 2001. MRBAYES: Bayesian inference of phylogeny.
507 Bioinformatics 17, 754–755.
508 Huson, D.H., Bryant, D., 2006. Application of phylogenetic networks in evolutionary studies. Mol.
509 Biol. Evol. 23, 254–267.
510 Irwin, D.M., Kocher, T.D., Wilson A.C., 1991. Evolution of the cytochrome b gene of mammals. J.
511 Mol. Evol. 32, 128–144.
512 Lanfear, R., Calcott, B., Ho, S.Y.W., Guindon, S., 2012. PartitionFinder: combined selection of
513 partitioning schemes and substitution models for phylogenetic analyses. Mol. Biol. Evol. 29,
514 1695–1701.

515 Leaché, A.D., Koo, M.S., Spencer, C.L., Papenfuss, T.J., Fisher, R.N., McGuire, J.A., 2009.
516 Quantifying ecological, morphological, and genetic variation to delimit species in the coast
517 horned lizard species complex (*Phrynosoma*). Proc Natl Acad Sci USA 106, 12418–12423.
518 Librado, P., Rozas, J., 2009. DNAsp v5: a software for comprehensive analysis of polymorphism
519 DNA data. Bioinformatics 25, 1451–1452.
520 Liu, L., Yu, L., Edwards, S.V., 2010. A maximum pseudo-likelihood approach for estimating
521 species trees under the coalescent model. BMC Evol. Biol. 10, 302.
522 Martín, C., Sanchiz, B., 2014. Lisanfos KMS. Version 1.2. Online reference accessible at
523 http://www.lisanfos.mncn.csic.es/. Museo Nacional de Ciencias Naturales, CSIC. Madrid,
524 Spain. Accessed July 21 2014.
525 Martínez-Solano, I., Teixeira, J., Buckley, D., García-París, M., 2006. Mitochondrial DNA
526 phylogeography of *Lissotriton boscai* (Caudata, Salamandridae): evidence for old, multiple
527 refugia in an Iberian endemic. Molecular Ecology 15, 3375–3388.
528 Martínez-Solano, Í., Peralta-García, A., Jockusch, E.L., Wake, D.B., Vázquez-Domínguez, E.,
529 Parra-Olea, G., 2012. Molecular systematics of *Batrachoseps* (Caudata, Plethodontidae) in
530 southern California and Baja California: mitochondrial-nuclear DNA discordance and the
531 evolutionary history of *B. major*. Molecular Phylogenetics and Evolution 63, 131–149.
532 Milne, I., Wright, F., Rowe, G., Marshall, D.F., Husmeier, D., McGuire, G., 2004. TOPALi:
533 software for automatic identification of recombinant sequences within DNA multiple
534 alignments. Bioinformatics 20, 1806–1807.
535 Moritz, C., Schneider, C.J., Wake, D.B., 1992. Evolutionary relationships within the *Ensatina*
536 *eschscholtzii* complex confirm the ring species interpretation. Syst. Biol. 41, 273-291.
537 Pargana, J. M. 1998. Características espectrais e temporais e correlações genéticas do canto de
538 acasalamento de *Pelodytes punctatus* (Amphibia, Anura). Masters Thesis. Departamento de
539 Biofísica. Universidade de Lisboa.163 pp.

Pargana, J.M., Marquez, R., Reques, R., Sánchez Herráiz, M.J., Tejedo, M., Crespo, E.G., 2003. The mating call of *Pelodytes ibericus* (Anura, Pelodytidae). Herpetological Journal 13, 199–204.

Pinho, C., Rocha, S., Carvalho, B.M., Lopes, S., Mourao, S., Vallinoto, M., Brunes, T.O., Haddad, C.F.B., Gonçalves, H., Sequeira, F., 2010. New primers for the amplification and sequencing of nuclear loci in a taxonomically wide set of reptiles and amphibians. Conserv. Genet. Resour. 2, 181–185.

Prychitko, T.M., Moore, W.S., 1997. The utility of DNA sequences of an intron from the b-fibrinogen gene in phylogenetic analysis of woodpeckers (Aves: Picidae). Mol. Phylogenet. Evol. 8, 193–204.

Puillandre, N., Modica, M.V., Zhang, Y., Sirovich, L., Boisselier, M.C., Cruaud, C., Holford, M., Samadi, S., 2012. Large-scale species delimitation method for hyperdiverse groups. Molecular Ecology 21, 2671–2691.

Rambaut, A., Suchard, M.A., Xie, D., Drummond, A.J., 2014. Tracer v1.6. Available from http://beast.bio.ed.ac.uk/Tracer. Accessed Nov. 28 2014.

Ramos-Onsins, S.E., Rozas, J., 2002. Statistical properties of new neutrality tests against population growth. Mol. Biol. Evol. 19, 2092-2100.

Recuero, E., Canestrelli, D., Vörös, J., Szabó, K., Poyarkov, N.A., Arntzen, J.W., Crnobrnja-Isailović, J., Kidov, A.A., Cogalniceanu, D., Caputo, F.P., Nascetti, G., Martínez-Solano, I., 2012. Multilocus species tree analyses resolve the radiation of the widespread *Bufo bufo* species group (Anura, Bufonidae). Molecular Phylogenetics and Evolution 62, 71–86.

Reis, D.M., Cunha, R.L., Patrão, C., Rebelo, R., Castilho, R., 2011. *Salamandra salamandra* (Amphibia: Caudata: Salamandridae) in Portugal: not all black and yellow. Genetica 139, 1095–1105.

564 Rivera, P.C., Di Cola, V., Martínez, J.J., Gardenal, C.N., Chiaraviglio, M., 2011. Species
565 delimitation in the continental forms of the genus *Epicrates* (Serpentes, Boidae) integrating
566 phylogenetics and environmental niche models. PLoS ONE 6, e22199.
567 Rogers, A.R., Harpending H., 1992. Population growth makes waves in the distribution of pairwise
568 genetic differences. Mol. Biol. Evol. 9, 552-569.
569 Ronquist, F., Teslenko, M., van der Mark, P., Ayres, D.L., Darling, A., Hohna, S., Larget, B., Liu,
570 L., Suchard, M.A., Huelsenbeck, J.P., 2012. MrBayes 3.2: efficient Bayesian phylogenetic
571 inference and model choice across a large model space. Syst. Biol. 61, 539–542.
572 Salzburger, W., Ewing, G.B., Von Haeseler, A., 2011. The performance of phylogenetic algorithms
573 in estimating haplotype genealogies with migration. Molecular Ecology 20,1952-1963.
574 Sambrook, J., Fritsch, E.F., Maniatis, T., 1989. Molecular Cloning: a Laboratory Manual, 2nd ed.
575 Cold Spring Harbor Press, New York.
576 Sánchez-Herráiz, M., Barbadillo, L., Machordom, A., Sanchiz, B., 2000. A new species of
577 pelodytid frog from the Iberian Peninsula. Herpetologica 56, 105–118.
578 Sanchiz, B., 1978. Nuevos restos fósiles de la familia Pelodytidae (Amphibia, Anura). Estudios
579 Geológicos, 34: 9-27.
580 Sanchiz, B., 1998. *Salientia. Handbuch der Paläoherpetologie Pars 4*. Dr. F. Pfeil, Munich.
581 Sanchiz, B., Tejedo, M., Sanchez-Herraiz, M., 2002. Osteological differentiation among Iberian
582 *Pelodytes* (Anura, Pelodytidae). Graellsia 58, 35–68.
583 Sequeira, F., Ferrand, N., Harris, D., 2006. Assessing the phylogenetic signal of the nuclear b-
584 fibrinogen intron 7 in salamandrids (Amphibia: Salamandridae). Amphibia-Reptilia 27,
585 409–418.
586 Sequeira, F., Sodre, D., Ferrand, N., Bernardi, J.A.R., Sampaio, I., Schneider, H., Vallinoto, M.,
587 2011. Hybridization and massive mtDNA unidirectional introgression between the closely
588 related Neotropical toads *Rhinella marina* and *R. schneideri* inferred from mtDNA and
589 nuclear markers. BMC Evol Biol 11, 264.

590 Shaw, T., Ruan, Z., Glenn, T., Liu, L., 2013. STRAW: Species TRee Analysis Web server. Nucleic
591 Acids Research 41, W238-241.
592 Silvestro, D., Michalak, I., 2010. RAxML GUI: a graphical front-end for RAML. Available at:
593 <http://sourceforge.net/projects/raxmlgui/>.
594 Sousa-Neves, T., Aleixo, A., Sequeira, F., 2013. Cryptic patterns of diversification of a widespread
595 Amazonian woodcreeper species complex (Aves: Dendrocolaptidae) inferred from
596 multilocus phylogenetic analysis: implications for historical biogeography and taxonomy.
597 Molecular Phylogenetics and Evolution 68, 410–424.
598 Stamatakis, A., 2006. RAxML-VI-HPC: maximum likelihood-based phylogenetic analyses with
599 thousands of taxa and mixed models. Bioinformatics 22, 2688–2690.
600 Stephens, M., Smith, N., Donnelly, P., 2001. A new statistical method for haplotype reconstruction
601 from population data. Am. J. Hum. Genet. 68, 978–989.
602 Stephens, M., Donnelly, P., 2003. A comparison of Bayesian methods for haplotype reconstruction
603 from population genotype data. Am. J. Hum. Genet. 73, 1162–1169.
604 Stöck, M., Dufresnes, C., Litvinchuk, S.N., Lymberakis, P., Biollay, S., Berroneau, M., Borzée, A.,
605 Ghali, K., Ogielska, M., Perrin, N., 2012. Cryptic diversity among Western Palearctic tree
606 frogs: postglacial range expansion, range limits, and secondary contacts of three European
607 tree frog lineages (*Hyla arborea* group). Molecular Phylogenetics and Evolution 65, 1–9.
608 Tajima, F., 1989. Statistical-method for testing the neutral mutation hypothesis by DNA
609 polymorphism. Genetics 123, 585-595.
610 Tamura, K., Stecher, G., Peterson, D., Filipski, A., Kumar, S., 2013. MEGA6: molecular
611 evolutionary genetics analysis version 6.0. Mol. Biol. Evol. 30, 2725–2729.
612 van de Vliet, M.S., Beebee, T.J., Diekmann, O.E., 2012. Genetic evidence for a distinct *Pelodytes*
613 lineage in southwest Portugal: implications for the use of pre-developed microsatellite
614 markers. Conserv. Genet. 13, 605–611.

615 Veith, M., Fromhage, L., Kosuch, J., Vences, M., 2006. Historical biogeography of Western
616 Palaearctic pelobatid and pelodytid frogs: a molecular phylogenetic perspective.
617 Contributions to Zoology 75, 109–120.
618 Vences, M., Wake, D.B., 2007. Speciation, species boundaries and phylogeography of amphibians.
619 In: Heatwhole and Tyler (eds.), Amphibian Biology, Vol. 7. Systematics. Surrey Beatty &
620 Sons, Australia, pp. 2613-2671.
621 Villesen, P., 2007. FaBox: an online toolbox for fasta sequences. Molecular Ecology Notes 7, 965–
622 968.
623 Watterson, G.A., 1975. On the number of segregating sites in genetical models without
624 recombination. Theor. Pop. Biol. 7, 256–276.
625 Weisrock, D.W., Rasoloarison, R.M., Fiorentino, I., Ralison, J.M., Goodman, S.M., Kappeler, P.M.,
626 Yoder, A.D., 2010. Delimiting species without nuclear monophyly in Madagascar's mouse
627 lemurs. PLoS ONE 5, e9883.
628 Weiss, S., Ferrand, N., 2007. Phylogeography of Southern European Refugia. Springer,
629 Netherlands.
630 Wiens, J.J., 2007. Species delimitation: new approaches for discovering diversity. Syst Biol 56,
631 875–878.
632 Zwickl, D.J., 2006. Genetic Algorithm Approaches for the Phylogenetic Analysis of Large
633 Biological Sequence Datasets Under the Maximum Likelihood Criterion. Ph.D. dissertation,
634 The University of Texas at Austin.

Fig. 1. Location of the 160 populations of *Pelodytes* sampled. Red- lineage A; yellow- lineage B (*P. ibericus*); green- lineage C; and blue- lineage D. The different background colors represent IUCN ranges for *P. punctatus* (blue) and *P. ibericus* (yellow). Insets show details of putative secondary contact zones.

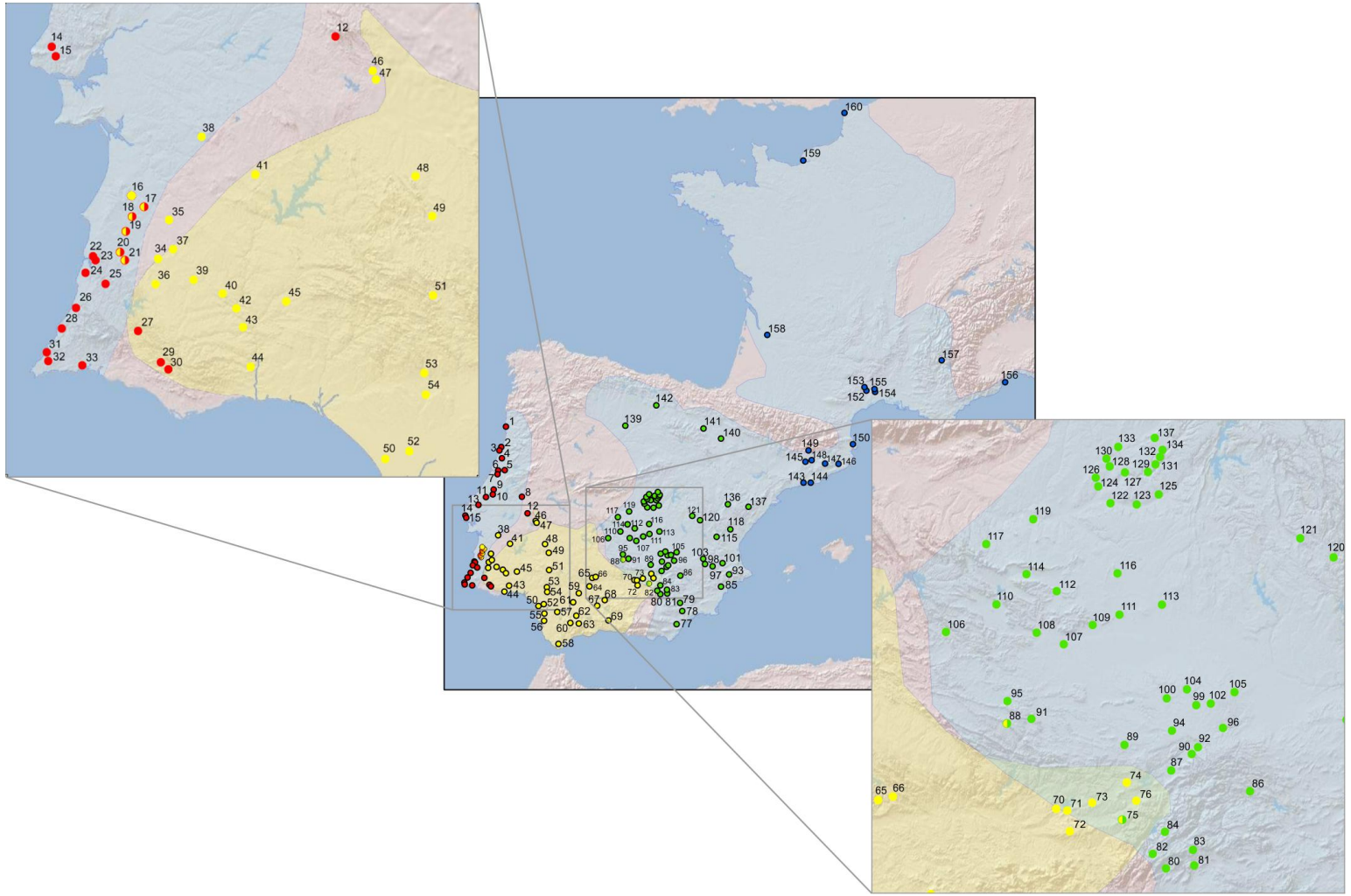

Fig. 2. Bayesian tree showing relationships between haplotypes in the combined mtDNA dataset. Colors as in Fig. 1. Values next to nodes are Bayesian posterior probabilities (BPP).

642 **Fig. 3**. Haplotype genealogy from maximum-likelihood analysis of mtDNA, *β-fibint7* and *PPP3CAint3* performed with the software Haploviewer.
643 Colors represent the different mtDNA clades (labeled A-D as in Figs. 1 and 2, see text for details). Each circle represents a different haplotype and its
644 size is proportional to its relative frequency. Dots represent inferred unsampled or extinct haplotypes.

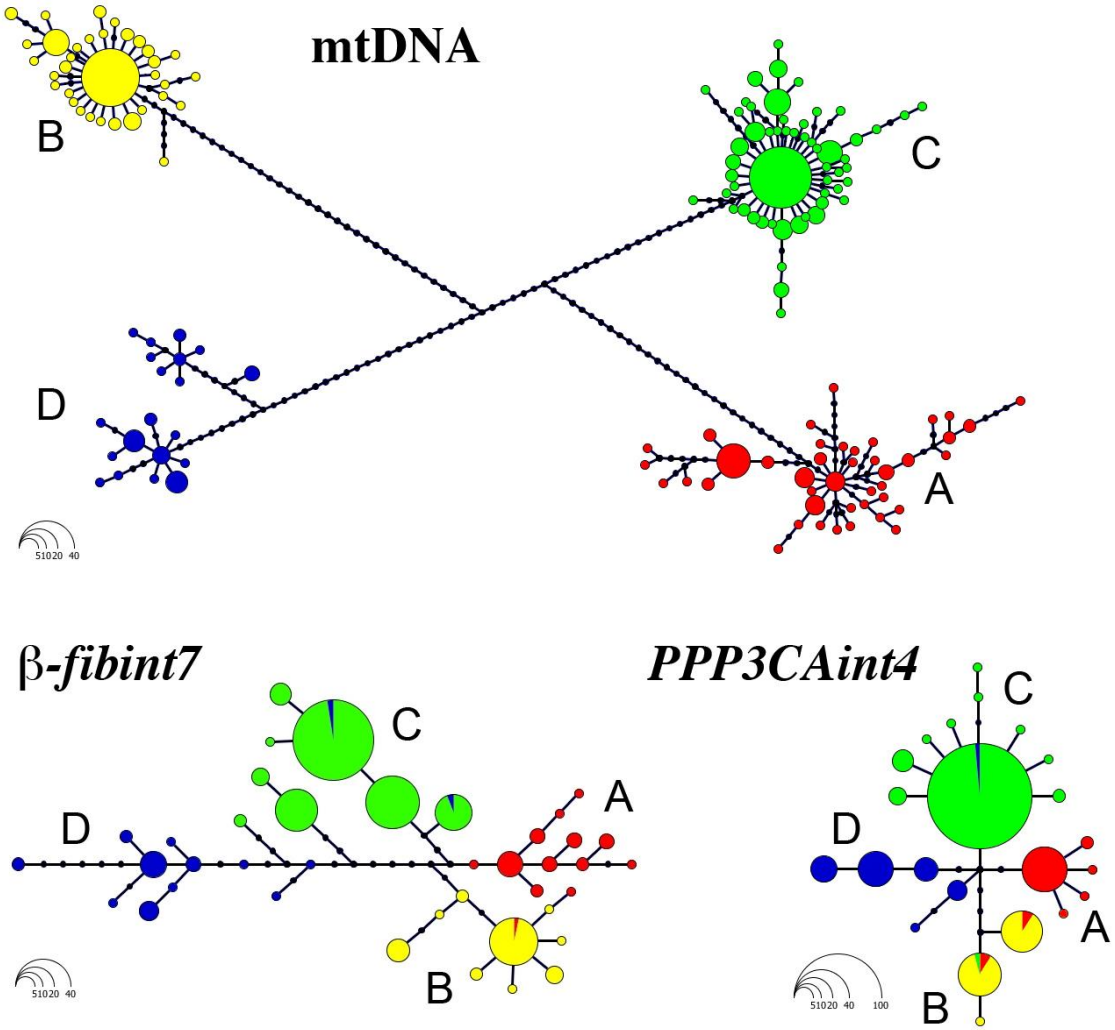

645

Fig. 4. Species tree of *Pelodytes*. Maximum clade credibility tree recovered by *BEAST, showing 95% highest posterior density intervals for split times (bars) and posterior probabilities for each node. Also shown are values of bootstrap support (in %) recovered in MP-EST analyses. Scale (bottom) in millions of years.

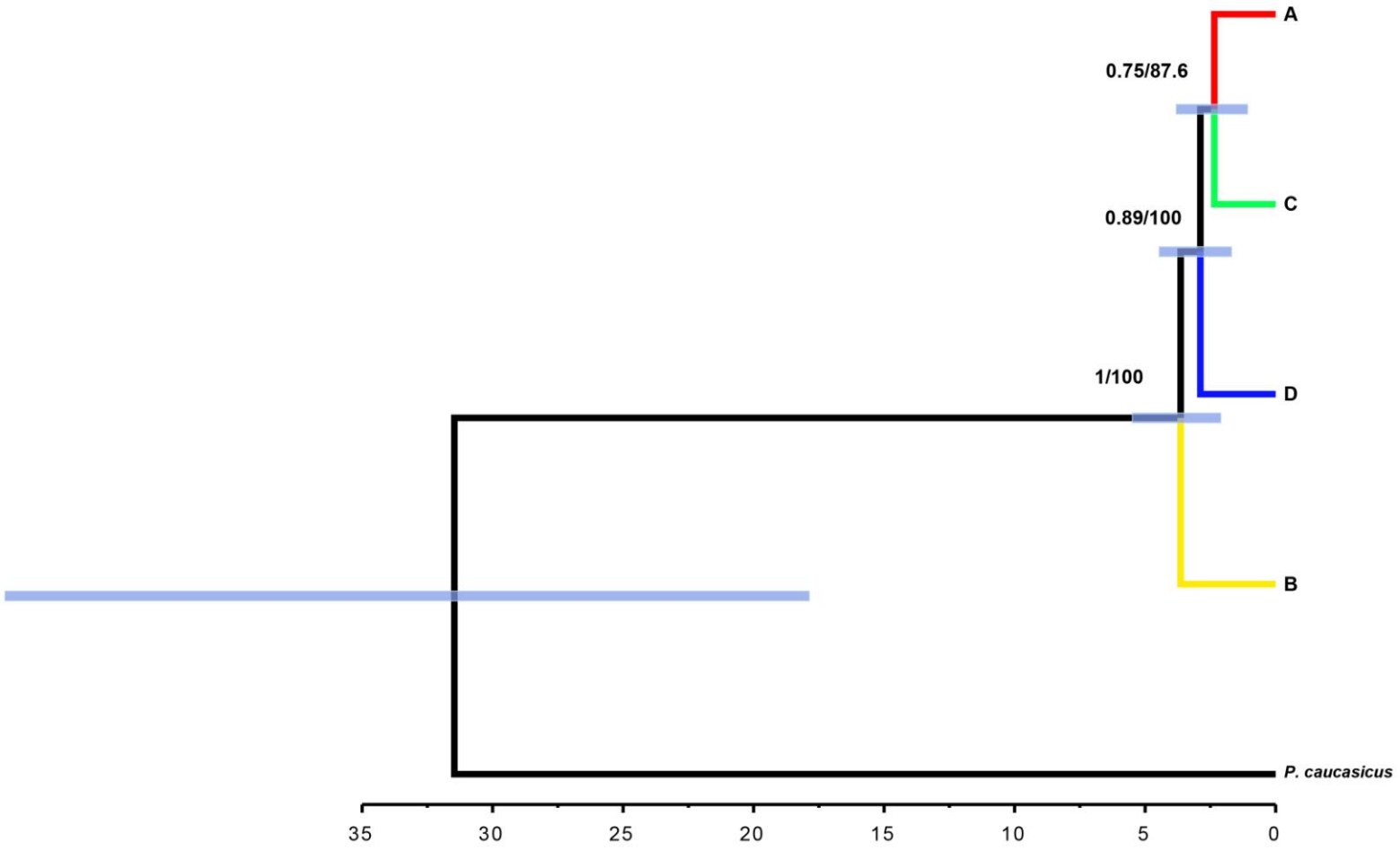

Fig. S1. Mismatch distribution plots for each mtDNA lineage in *Pelodytes*. The blue curve shows the distribution of the observed pairwise nucleotide site differences and red curves the expected values in growing and declining populations.

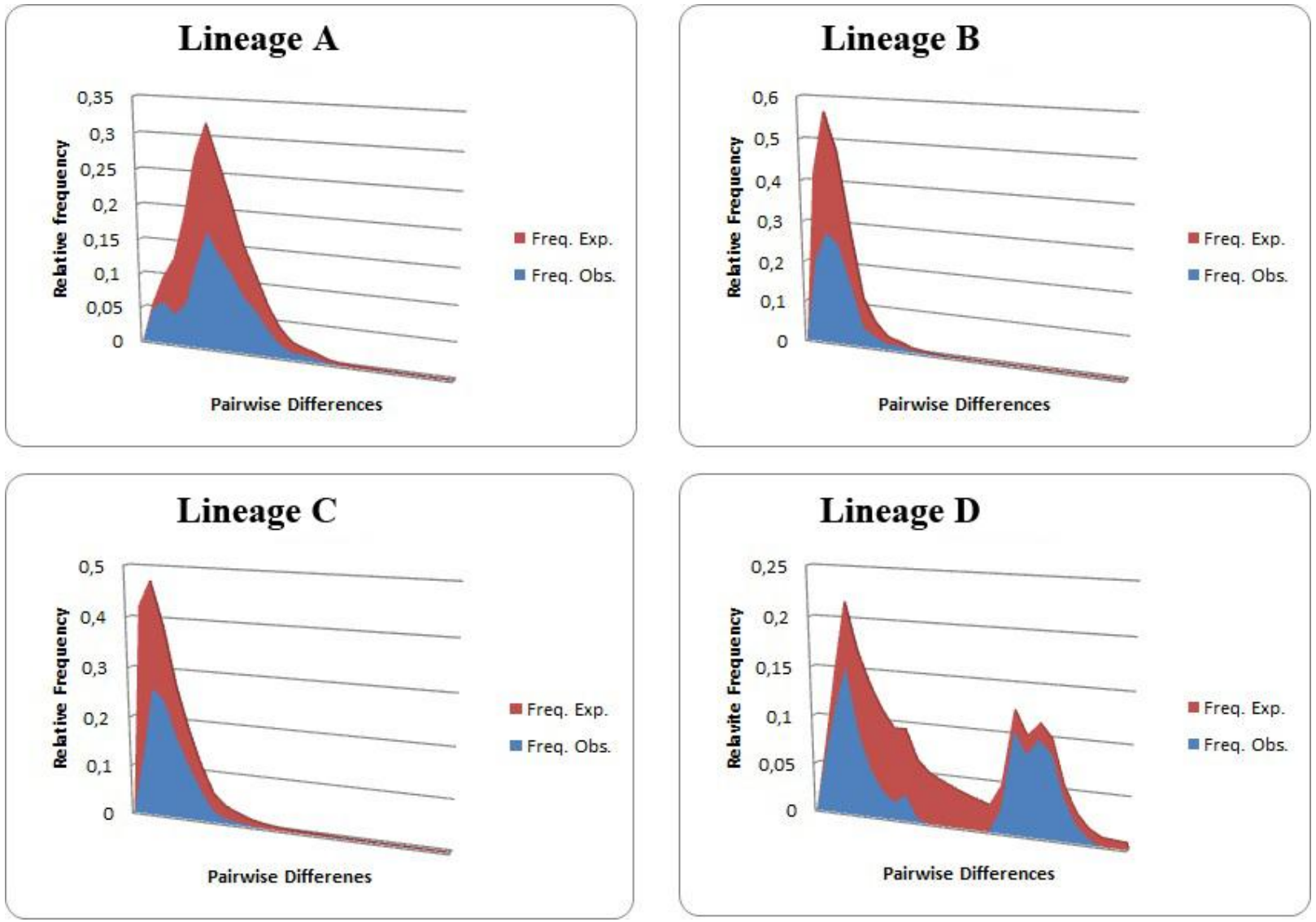

Tables

Table 1. Sample information: ID_POP as in Fig. 1 (an asterisk marks sympatry of two different mtDNA clades), sample code, mtDNA haplotype clade, locality, country, latitude and longitude and GenBank accession numbers for newly generated sequences. The "Observations" field highlights instances of cyto-nuclear discordance (based on discordance between gene trees).

ID_POP	Sample Code	mtDNA	Locality	Country	Latitude	Longitude	*cob*	*nad4*	*β-fibint7*	*PPP3CAint4*	Observations
1	MIN01	A	Mindelo	Portugal	41,30	-8,71	KP166542	KP166909		KP166142-KP166143	
	MIN02	A	Mindelo	Portugal	41,30	-8,71	KP166543	KP166910			
2	Torr	-	Murtosa, Portugal	Portugal	40,76	-8,71				KP166154-KP166155	
3	IMS4630	A	São Jacinto	Portugal	40,67	-8,74	KP166535	KP166902			
	IMS4631	A	São Jacinto	Portugal	40,67	-8,74	KP166536	KP166903			
4	BUS03	A	Bustos, Oliveira do Bairro	Portugal	40,49	-8,61	KP166514	KP166881			
5	Coimbra	A	Coimbra	Portugal	40,21	-8,43	KP166518	KP166885	KP165852-KP165853	KP166136-KP166137	
6	Svarao	A	Santo Varão, Montemor-o-Velho	Portugal	40,18	-8,60	KP166570	KP166937			
7	SOU01	A	Soure	Portugal	40,06	-8,63	KP166568	KP166935	KP165868-KP165869		
	Soure	A	Soure	Portugal	40,06	-8,63	KP166569	KP166936			
8	SAL01	A	Salgueiral, Vila-Velha-de-Ródão	Portugal	39,65	-7,67	KP166561	KP166928	KP165862-KP165863		
	SAL02	A	Salgueiral, Vila-Velha-de-Ródão	Portugal	39,65	-7,67	KP166562	KP166929	KP165864-KP165865		

9	IMS4624	A	Rexaldia	Portugal	39,57	-8,53	KP166534	KP166901			
	IMS4639	A	Granja do Ulmeiro, Rio Mondego	Portugal	40,16	-8,64	KP166537	KP166904			
	IMS4640	A	Granja do Ulmeiro, Rio Mondego	Portugal	40,16	-8,64	KP166538	KP166905			
10	IMS4618	A	Mosteiro de Alcanena	Portugal	39,42	-8,84	KP166532	KP166899			
	IMS4619	A	Mosteiro de Alcanena	Portugal	39,42	-8,84	KP166533	KP166900			
11	SAires01	A	Serra de Aires	Portugal	39,56	-8,58	KP166559	KP166926		KP166148-KP166149	
	SAires02	A	Serra de Aires	Portugal	39,56	-8,58	KP166560	KP166927			
	SAires03	-	Serra de Aires	Portugal	39,56	-8,58			KP165866-KP165867	KP166152-KP166153	
12	IMS4614	A	Alpalhão	Portugal	39,27	-7,38	KP166527	KP166894			
	IMS4615	A	Alpalhão	Portugal	39,27	-7,38	KP166528	KP166895			
	IMS4616	A	Alpalhão	Portugal	39,27	-7,38	KP166529	KP166896			
	IMS4617a	A	Alpalhão	Portugal	39,27	-7,38	KP166530	KP166897			
	IMS4617b	A	Alpalhão	Portugal	39,27	-7,38	KP166531	KP166898			
13	IMS2893	-	Montejunto	Portugal	39,17	-9,02			KP165872-KP165873	KP166126-KP166127	
	IMS2894	A	Montejunto	Portugal	39,17	-9,02	KP166526	KP166893	KP165874-KP165875	KP166128-KP166129	
14	IMS2870	-	Sintra-Mafra	Portugal	38,83	-9,36			KP165846-KP165847	KP166124-KP166125	
	IMS2871	-	Sintra-Mafra	Portugal	38,83	-9,36			KP165848-KP165849		
15	CA15	A	Cacém	Portugal	38,78	-9,31	KP166515	KP166882	KP165870-KP165871		

16	CID03	B	Cidrão, Mosqueirões, Grândola	Portugal	38,12	-8,56	KP166426	KP166793			
	CID06	B	Cidrão, Mosqueirões, Grândola	Portugal	38,12	-8,56	KP166427	KP166794			
17*	GRA03	B	Grândola	Portugal	38,08	-8,46	KP166438	KP166805			
	GRA04	B	Grândola	Portugal	38,08	-8,46	KP166439	KP166806			
	GRA06	A	Grândola	Portugal	38,08	-8,46	KP166524	KP166891			
	Grando08	A	Grândola	Portugal	38,08	-8,46	KP166525	KP166892	KP165854-KP165855	KP166138-KP166139	Cyto-nuclear discordance (*β-fibint7* and *PPP3CAint4)*
18*	OLO21	A	Outeiro do Lobo	Portugal	38,01	-8,53	KP166546	KP166913	KP165858-KP165859	KP166144-KP166145	Cyto-nuclear discordance (*β-fibint7* and *PPP3CAint4*)
	OLO18	B	Outeiro do Lobo	Portugal	38,01	-8,53	KP166470	KP166837			
	OLO20	B	Outeiro do Lobo	Portugal	38,01	-8,53	KP166471	KP166838		KP166192-KP166193	
	OLO22	-	Outeiro do Lobo	Portugal	38,01	-8,53				KP166146-KP166147	
19*	XAU01	A	Vale de Água	Portugal	37,92	-8,55	KP166578	KP166945		KP166156-KP166157	
	XAU02	A	Vale de Água	Portugal	37,92	-8,55	KP166579	KP166946			
	XAU04	B	Vale de Água	Portugal	37,92	-8,55	KP166498	KP166865			
20*	CBS01	A	Campo Redondo	Portugal	37,80	-8,56	KP166516	KP166883			
	CBS02	A	Campo Redondo	Portugal	37,80	-8,56	KP166517	KP166884			
	BICD3	-	Campo Redondo	Portugal	37,80	-8,55				KP166132-KP166133	
	BICD5	-	Campo Redondo	Portugal	37,80	-8,55				KP166134-KP166135	
	BICD6	A	Campo Redondo	Portugal	37,80	-8,55	KP166506	KP166873			

	BICD7	A	Campo Redondo	Portugal	37,80	-8,55	KP166507	KP166874			
	BICD8	B	Campo Redondo	Portugal	37,80	-8,55	KP166421	KP166788			
	BICD9	A	Campo Redondo	Portugal	37,80	-8,55	KP166508	KP166875			
	COLF2	A	Campo Redondo	Portugal	37,78	-8,56	KP166519	KP166886			
	COLF3	A	Campo Redondo	Portugal	37,78	-8,56	KP166520	KP166887			
	COLF5	A	Campo Redondo	Portugal	37,78	-8,56	KP166521	KP166888			
	COLF4	B	Campo Redondo	Portugal	37,78	-8,56	KP166430	KP166797			
21*	SOL03	A	Soalheira, Campo Redondo	Portugal	37,76	-8,51	KP166566	KP166933		KP166198-KP166199	Cyto-nuclear discordance (*PPP3CAint4*) (clades A+B)
	SOL04	A	Soalheira, Campo Redondo	Portugal	37,76	-8,51	KP166567	KP166934			
	SOL01	B	Soalheira, Campo Redondo	Portugal	37,76	-8,51	KP166488	KP166855			
22	VMF49	A	Vila Nova de Milfontes	Portugal	37,74	-8,74	KP166577	KP166944			
23	SLU40	A	Vila Nova de Milfontes	Portugal	37,72	-8,71	KP166565	KP166932			
	SLU01	A	Vila Nova de Milfontes	Portugal	37,72	-8,71	KP166563	KP166930			
	SLU02	A	Vila Nova de Milfontes	Portugal	37,72	-8,71	KP166564	KP166931			
	SLU06	-	Vila Nova de Milfontes	Portugal	37,72	-8,71				KP166150-KP166151	
	VMF01	A	Vila Nova de Milfontes	Portugal	37,72	-8,77	KP166574	KP166941			
	VMF02	A	Vila Nova de Milfontes	Portugal	37,72	-8,77	KP166575	KP166942			
	VMF03	A	Vila Nova de Milfontes	Portugal	37,72	-8,77	KP166576	KP166943			
24	ALM25b	A	Cavaleiros	Portugal	37,67	-8,79	KP166505	KP166872			
	CVL01	A	Cavaleiros	Portugal	37,64	-8,76	KP166522	KP166889			
	CVL03	A	Cavaleiros	Portugal	37,64	-8,76	KP166523	KP166890			
25	BMP01	A	Bemposta	Portugal	37,60	-8,61	KP166509	KP166876			
	BMP03	A	Bemposta	Portugal	37,60	-8,61	KP166510	KP166877			

	BMP05	A	Bemposta	Portugal	37,60	-8,61	KP166511	KP166878			
26	PAC401	A	Odeceixe	Portugal	37,43	-8,78	KP166547	KP166914			
	PAC402	A	Odeceixe	Portugal	37,43	-8,78	KP166548	KP166915			
	PAC403	A	Odeceixe	Portugal	37,43	-8,78	KP166549	KP166916			
27	BRR01	A	Barreiros, Boião	Portugal	37,39	-8,31	KP166512	KP166879			
	BRR03	A	Barreiros, Boião	Portugal	37,39	-8,31	KP166513	KP166880			
28	ALJ01	-	Aljezur	Portugal	37,30	-8,84				KP166130-KP166131	
	ALJ02	A	Aljezur	Portugal	37,30	-8,84	KP166503	KP166870	KP165850-KP165851		
	ALJ03	A	Aljezur	Portugal	37,30	-8,84	KP166504	KP166871			
	TEL07	A	Vale de Telha	Portugal	37,30	-8,84	KP166571	KP166938			
	TEL08	A	Vale de Telha	Portugal	37,30	-8,84	KP166572	KP166939			
	LAG312	A	Aljezur	Portugal	37,31	-8,81	KP166539	KP166906			
	LAG313	A	Aljezur	Portugal	37,31	-8,81	KP166540	KP166907			
29	PEN31	A	Penina	Portugal	37,25	-8,11	KP166550	KP166917			
	PEN32	A	Penina	Portugal	37,25	-8,11	KP166551	KP166918			
	RDP03	A	Rocha de Pena	Portugal	37,25	-8,10	KP166554	KP166921	KP165860-KP165861		
	RDP04	A	Rocha de Pena	Portugal	37,25	-8,10	KP166555	KP166922			
30	NDB40	A	Nave do Barão	Portugal	37,22	-8,05	KP166544	KP166911			
	NDB41	A	Nave do Barão	Portugal	37,22	-8,05	KP166545	KP166912			
31	PFU212	A	Pena Furada	Portugal	37,15	-8,91	KP166552	KP166919			
	PFU213	A	Pena Furada	Portugal	37,15	-8,91	KP166553	KP166920			
32	VDB47	A	Vila do Bispo	Portugal	37,10	-8,88	KP166573	KP166940			

	ROR91	A	Vila do Bispo	Portugal	37,11	-8,91	KP166556	KP166923			
	ROR92	A	Vila do Bispo	Portugal	37,11	-8,91	KP166557	KP166924			
	ROR93	A	Vila do Bispo	Portugal	37,11	-8,91	KP166558	KP166925			
33	Lagos	A	Lagos	Portugal	37,12	-8,65	KP166541	KP166908	KP165856-KP165857	KP166140-KP166141	
34	AEL23	B	Aldeia dos Elvas, Aljustrel	Portugal	37,81	-8,28	KP166410	KP166777			
	AEL24	B	Aldeia dos Elvas, Aljustrel	Portugal	37,81	-8,28	KP166411	KP166778			
35	CAH05	B	Canhestros	Portugal	38,04	-8,27	KP166422	KP166789			
36	OUR09	B	Ourique	Portugal	37,72	-8,30	KP166473	KP166840			
	OUR16	B	Ourique	Portugal	37,67	-8,26	KP166474	KP166841			
	OUR18	B	Ourique	Portugal	37,67	-8,26	KP166475	KP166842			
37	RMO32	B	Rio de Moinhos, Aljustrel	Portugal	37,89	-8,19	KP166480	KP166847	KP165904-KP165905	KP166194-KP166195	
	RMO33	B	Rio de Moinhos, Aljustrel	Portugal	37,89	-8,19	KP166481	KP166848			
38	ESC01	B	Santiago do Escoural	Portugal	38,54	-8,17	KP166433	KP166800			
	ESC02	B	Santiago do Escoural	Portugal	38,54	-8,17	KP166434	KP166801	KP165898-KP165899		
39	CAV01	B	Castro Verde	Portugal	37,74	-8,01	KP166423	KP166790			
	CAV77	B	Castro Verde	Portugal	37,74	-8,01	KP166424	KP166791			
	CAV78	B	Castro Verde	Portugal	37,74	-8,01	KP166425	KP166792			
40	ARU16	B	Alcaira Ruiva, Mértola	Portugal	37,71	-7,79	KP166415	KP166782			
	ARU17	B	Alcaira Ruiva, Mértola	Portugal	37,71	-7,79	KP166416	KP166783			
41	RMT1	B	Monte do Trigo	Portugal	38,40	-7,73	KP166482	KP166849			
42	ME02	B	Mértola	Portugal	37,64	-7,57	KP166464	KP166831			
43	IMS2881	B	Sedas	Portugal	37,54	-7,60	KP166453	KP166820	KP165888-	KP166164-	

									KP165889	KP166165	
	IMS2882	B	Sedas	Portugal	37,54	-7,60	KP166454	KP166821	KP165922-KP165923	KP166166-KP166167	
44	ODE2023	B	Odeleite	Portugal	37,34	-7,49	KP166469	KP166836	KP165876-KP165877	KP166158-KP166159	
	ALO02	B	Almada de Ouro	Portugal	37,34	-7,49	KP166412	KP166779	KP165890-KP165891	KP166170-KP166171	
45	PAY2032	B	Paymogo	Spain	37,75	-7,33	KP166478	KP166845	KP165878-KP165879		
46	GLB01	B	Los Barros	Spain	39,13	-7,06	KP166435	KP166802		KP166178-KP166179	
	GLB02	B	Los Barros	Spain	39,13	-7,06	KP166436	KP166803			
	GLB03	B	Los Barros	Spain	39,13	-7,06	KP166437	KP166804			
47	NSE02	B	Ouguela	Portugal	39,08	-7,03	KP166468	KP166835			
48	SMB02	B	Santa Marta de Barros	Spain	38,60	-6,61	KP166487	KP166854			
49	ZFR01	B	Zafra	Spain	38,40	-6,44	KP166501	KP166868			
	ZFR02	B	Zafra	Spain	38,40	-6,44	KP166502	KP166869			
50	EBD55	B	Parque Nacional de Doñana	Spain	37,00	-6,44	KP166432	KP166799	KP165892-KP165893		
51	CJA04	B	Campo de Javata, Cala	Spain	37,96	-6,32	KP166429	KP166796			
	CJA03	B	Campo de Javata, Cala	Spain	37,96	-6,32	KP166428	KP166795			
52	IB32	B	PN Doñana	Spain	37,07	-6,28	KP166444	KP166811	KP165910-KP165911	KP166180-KP166181	
	IB35	B	PN Doñana	Spain	37,07	-6,28	KP166445	KP166812	KP165912-KP165913	KP166182-KP166183	

	IBH1	B	PN Doñana	Spain	37,07	-6,28	KP166446	KP166813	KP165900-KP165901		
	IBH2	B	PN Doñana	Spain	37,07	-6,28	KP166447	KP166814	KP165914-KP165915	KP166184-KP166185	
	IBL4	B	PN Doñana	Spain	37,07	-6,28	KP166448	KP166815	KP165916-KP165917	KP166186-KP166187	
	IBL5	B	PN Doñana	Spain	37,07	-6,28	KP166449	KP166816	KP165902-KP165903		
53	AZN157	-	Aznalcollar	Spain	37,52	-6,28				KP166172-KP166173	
54	CQU01	B	Casa Quemada, Sanlucar la Mayor	Spain	37,40	-6,24	KP166431	KP166798			
55	TRE185	B	Salida A-471. Trebujena	Spain	36,84	-6,20	KP166495	KP166862			
	TRE02	B	Salida A-471. Trebujena	Spain	36,86	-6,19	KP166492	KP166859			
	TRE13	B	Salida A-471. Trebujena	Spain	36,86	-6,19	KP166493	KP166860			
	TRE14	B	Salida A-471. Trebujena	Spain	36,86	-6,19	KP166494	KP166861			
56	JER01	B	Jerez	Spain	36,66	-6,17	KP166461	KP166828			
	JER02	B	Jerez	Spain	36,66	-6,17	KP166462	KP166829			
	JER12	B	Jerez	Spain	36,66	-6,17	KP166463	KP166830	KP165918-KP165919	KP166188-KP166189	
57	ATA01	B	Montellano	Spain	36,95	-5,81	KP166417	KP166784		KP166168-KP166169	
	ATA02	B	Montellano	Spain	36,95	-5,81	KP166418	KP166785			
58	POJ27	B	Pista Ojén	Spain	36,15	-5,59	KP166479	KP166846			
59	IMS2868	B	Marchena-Puebla de Cazalla	Spain	37,28	-5,37	KP166450	KP166817	KP165882-KP165883	KP166160-KP166161	

	IMS2869	B	Marchena-Puebla de Cazalla	Spain	37,28	-5,37	KP166451	KP166818	KP165884-KP165885	KP166162-KP166163	
60	GRZ02	B	Grazalema	Spain	36,74	-5,34	KP166440	KP166807			
	GRZ04	B	Grazalema	Spain	36,74	-5,34	KP166441	KP166808			
	GRZ10	B	Grazalema	Spain	36,74	-5,34	KP166442	KP166809			
61	IMS2880	B	Puebla de Cazalla	Spain	37,17	-5,24	KP166452	KP166819	KP165886-KP165887		
62	OLV73	B	Olvera	Spain	36,95	-5,19	KP166472	KP166839			
63	RON23	B	Ronda	Spain	36,77	-5,08	KP166483	KP166850			
64	GUA41	B	Guadalcázar	Spain	37,76	-4,95	KP166443	KP166810			
65	TOB09	B	Toba	Spain	37,99	-4,90	KP166490	KP166857	KP165908-KP165909		
	TOB10	B	Toba	Spain	37,99	-4,90	KP166491	KP166858	KP165920-KP165921		
66	IMS4425	B	Estación de Obejo	Spain	38,03	-4,80	KP166455	KP166822			
	IMS4426	B	Estación de Obejo	Spain	38,03	-4,80	KP166456	KP166823			
67	TAR67	B	Taraje	Spain	37,32	-4,59	KP166489	KP166856	KP165894-KP165895	KP166174-KP166175	
68	IMS2863	-	Cabra	Spain	37,49	-4,38			KP165880-KP165881		
69	PAR101	B	Nac. Parrica	Spain	36,99	-4,16	KP166476	KP166843			
	PAR102	B	Nac. Parrica	Spain	36,99	-4,16	KP166477	KP166844			
	ZAF103	B	Zafarraya	Spain	36,99	-4,16	KP166499	KP166866			
	ZAF104	B	Zafarraya	Spain	36,99	-4,16	KP166500	KP166867			
	ZAF33	-	Zafarraya	Spain	36,99	-4,16				KP166202-	

										KP166203	
	ZAF82	-	Zafarraya	Spain	36,99	-4,16			KP165896-KP165897	KP166176-KP166177	
70	VIL163	B	Vilches	Spain	38,14	-3,54	KP166496	KP166863			
	VIL164	B	Vilches	Spain	38,14	-3,54	KP166497	KP166864			
	VIL182	-	Vilches	Spain	38,14	-3,54				KP166200-KP166201	
71	ARQ01	B	Arquillos	Spain	38,15	-3,46	KP166413	KP166780			
	ARQ02	B	Arquillos	Spain	38,15	-3,46	KP166414	KP166781			
72	JAE47	B	Úbeda	Spain	38,02	-3,41	KP166460	KP166827			
	51UBD	B	Úbeda	Spain	38,02	-3,39	KP166409	KP166776			
73	SAN45	B	Santisteban del Puerto	Spain	38,22	-3,28	KP166484	KP166851			
	SAN46	B	Santisteban del Puerto	Spain	38,22	-3,28	KP166485	KP166852			
	SAN49	B	Santisteban del Puerto	Spain	38,22	-3,28	KP166486	KP166853			
74	MON35	B	Montizón	Spain	38,38	-3,04	KP166466	KP166833			
	MON36	B	Montizón	Spain	38,38	-3,04	KP166467	KP166834			
75*	ISN1	B	Iznatoraf	Spain	38,15	-3,03	KP166457	KP166824	KP165906-KP165907	KP166196-KP166197	
	IZN228	B	Iznatoraf	Spain	38,15	-3,03	KP166459	KP166826			
	IZN222	C	Iznatoraf	Spain	38,15	-3,03	KP166672	KP167039			
	IZN01	B	Iznatoraf	Spain	38,15	-3,03	KP166458	KP166825			
76	BEAD11	B	Arroyo de Beas de Segura	Spain	38,28	-2,95	KP166419	KP166786			
	BEAD12	B	Arroyo de Beas de Segura	Spain	38,28	-2,95	KP166420	KP166787			
77	35BED01	C	Bedar	Spain	37,20	-1,99	KP166580	KP166947	KP166020-KP166021	KP166282-KP166283	

	35BED02	C	Bedar	Spain	37,20	-1,99	KP166581	KP166948			
78	AGU04	C	Águilas	Spain	37,56	-1,87	KP166588	KP166955			
	AGU05	C	Águilas	Spain	37,56	-1,87	KP166589	KP166956			
79	49LORC	C	Pozo en Rambla de las Fuentes, Lorca	Spain	37,76	-1,98	KP166582	KP166949	KP165978-KP165979	KP166284-KP166285	
80	ANI3059	-	Salida de las Ánimas	Spain	37,90	-2,64			KP165966-KP165967		
81	CAP3047	C	Cortijo El Capricho	Spain	37,95	-2,43	KP166609	KP166976	KP165962-KP165963		
82	CUE15	C	Cueva París	Spain	37,97	-2,76	KP166611	KP166978			
83	FBell	C	Fuente Bella	Spain	38,04	-2,46	KP166614	KP166981	KP165986-KP165987		
	FBell03	C	Fuente Bella	Spain	38,04	-2,46	KP166615	KP166982			
	FBell04	C	Fuente Bella	Spain	38,04	-2,46	KP166616	KP166983	KP165988-KP165989	KP166300-KP166301	
	POR3050	C	Salida Porcunas	Spain	38,00	-2,46	KP166688	KP167055	KP165964-KP165965		
84	ACDC01	C	Casas de Carrasco, Santiago de la Espada	Spain	38,12	-2,69	KP166586	KP166953			
	ACDC02	C	Casas de Carrasco, Santiago de la Espada	Spain	38,12	-2,69	KP166587	KP166954			
	CDC7324	C	Casas de Carrasco, Santiago de la Espada	Spain	38,13	-2,69	KP166610	KP166977			
85	IMS1958	C	Aspe	Spain	38,33	-0,73	KP166654	KP167021	KP165950-KP165951	KP166254-KP166255	
86	54ANCH	C	CM 412 Km 230, bajo la Anchura	Spain	38,45	-2,09	KP166583	KP166950			
87	VRO03	C	Villarrodrigo	Spain	38,50	-2,71	KP166726	KP167093		KP166362-KP166363	

	VRO04	C	Villarrodrigo	Spain	38,50	-2,71	KP166727	KP167094			
	VRO06	-	Villarrodrigo	Spain	38,50	-2,71				KP166364-KP166365	
	VRO07	-	Villarrodrigo	Spain	38,50	-2,71				KP166366-KP166367	
	VRO08	-	Villarrodrigo	Spain	38,50	-2,71				KP166368-KP166369	
	VRO09	-	Villarrodrigo	Spain	38,50	-2,71				KP166370-KP166371	
	VRT10	C	Laguna del Tiro. Villarrodrigo	Spain	38,49	-2,70	KP166728	KP167095			
	VRT11	C	Laguna del Tiro. Villarrodrigo	Spain	38,49	-2,70	KP166729	KP167096			
88*	Mest01	B	Mestanza	Spain	38,60	-4,02	KP166465	KP166832		KP166190-KP166191	Cyto-nuclear discordance (*PPP3CAint4*) (clades B+C)
	Mest02	C	Mestanza	Spain	38,60	-4,02	KP166683	KP167050	KP165994-KP165995	KP166314-KP166315	
	MES01	C	Mestanza	Spain	38,60	-4,02	KP166680	KP167047			
	MES02	C	Mestanza	Spain	38,60	-4,02	KP166681	KP167048			
	MES06	C	Mestanza	Spain	38,60	-4,02	KP166682	KP167049		KP166308-KP166309	
	MES07	-	Mestanza	Spain	38,60	-4,02				KP166310-KP166311	*PPP3CAint4* alleles clustering with clades B and C
89	CAD31	C	Torre de Juan Abad	Spain	38,60	-3,10	KP166601	KP166968			
	CAD32	C	Torre de Juan Abad	Spain	38,60	-3,10	KP166602	KP166969			
90	REO01	C	Reolid	Spain	38,62	-2,58	KP166714	KP167081			
91	CAL41	C	Campo de Calatrava	Spain	38,66	-3,84	KP166603	KP166970			

	CAL42	C	Campo de Calatrava	Spain	38,66	-3,84	KP166604	KP166971			
92	ALC27	C	Río Alcaraz, Albacete	Spain	38,66	-2,54	KP166590	KP166957			
	ALC28	C	Río Alcaraz, Albacete	Spain	38,66	-2,54	KP166591	KP166958			
	ALC29	C	Río Alcaraz, Albacete	Spain	38,66	-2,54	KP166592	KP166959			
93	IMS1941	C	Mas de Celedons	Spain	38,67	-0,52	KP166652	KP167019	KP165946-KP165947	KP166250-KP166251	
	IMS1942	C	Mas de Celedons	Spain	38,67	-0,52	KP166653	KP167020	KP165948-KP165949	KP166252-KP166253	
94	CANa90	C	Cañamares	Spain	38,74	-2,76	KP166605	KP166972			
	CANa91	C	Cañamares	Spain	38,74	-2,76	KP166606	KP166973			
	CANa92	C	Cañamares	Spain	38,74	-2,76	KP166607	KP166974			
	CANa93	C	Cañamares	Spain	38,74	-2,76	KP166608	KP166975			
	SMA06	C	Santa María	Spain	38,73	-2,74	KP166719	KP167086	KP166030-KP166031	KP166372-KP166373	
	SMA94	C	Santa María	Spain	38,73	-2,74	KP166720	KP167087			
	SMA95	C	Santa María	Spain	38,73	-2,74	KP166721	KP167088			
95	TIR01	C	Tirteafuera	Spain	38,74	-4,05	KP166722	KP167089		KP166360-KP166361	
	TIR02	C	Tirteafuera	Spain	38,74	-4,05	KP166723	KP167090			
	TIR03	C	Tirteafuera	Spain	38,74	-4,05	KP166724	KP167091			
	TIR04	C	Tirteafuera	Spain	38,74	-4,05	KP166725	KP167092			
96	VVE01	C	Villaverde	Spain	38,81	-2,37	KP166730	KP167097			
97	55LOS	C	Canal de Los Losares	Spain	38,82	-1,09	KP166584	KP166951	KP165980-KP165981	KP166286-KP166287	
98	56BON	C	Pozo cerca Cerro del Almarejo	Spain	38,85	-1,34	KP166585	KP166952	KP165982-		

									KP165983		
99	BON70	C	El Bonillo, Loma de Pelao	Spain	38,92	-2,60	KP166593	KP166960		KP166292-KP166293	
	BON71	C	El Bonillo, Loma de Pelao	Spain	38,92	-2,60	KP166594	KP166961			
	BON72	C	El Bonillo, Loma de Pelao	Spain	38,92	-2,60	KP166595	KP166962			
	57AYHOR	-	Arroyo de Los Horcajos	Spain	38,93	-2,58			KP166022-KP166023	KP166288-KP166289	
100	RUI62	C	Laguna Tinaja. Ruidera	Spain	38,93	-2,83	KP166715	KP167082			
	RUI63	C	Laguna Tinaja. Ruidera	Spain	38,93	-2,83	KP166716	KP167083			
	RUI64	C	Laguna Tinaja. Ruidera	Spain	38,93	-2,83	KP166717	KP167084			
	RUI65	C	Laguna Tinaja. Ruidera	Spain	38,93	-2,83	KP166718	KP167085			
101	IMS1881	C	Enguera	Spain	38,94	-0,79	KP166645	KP167012			
	IMS1882	C	Enguera	Spain	38,94	-0,79	KP166646	KP167013	KP165944-KP165945	KP166238-KP166239	
	IMS1889	C	Enguera	Spain	38,94	-0,79	KP166647	KP167014		KP166240-KP166241	
	IMS1890	C	Enguera	Spain	38,94	-0,79	KP166648	KP167015		KP166242-KP166243	
	IMS1891	C	Enguera	Spain	38,94	-0,79	KP166649	KP167016		KP166244-KP166245	
	IMS1892	C	Enguera	Spain	38,94	-0,79	KP166650	KP167017		KP166246-KP166247	
	IMS1893	C	Enguera	Spain	38,94	-0,79	KP166651	KP167018		KP166248-KP166249	
102	BON77	C	El Bonillo, Navazo de Navalcudia	Spain	38,94	-2,49	KP166596	KP166963			

	BON78	C	El Bonillo, Navazo de Navalcudia	Spain	38,94	-2,49	KP166597	KP166964			
	58PIC	-	Cañada de Picado o Losilla	Spain	38,90	-2,51			KP166024-KP166025	KP166290-KP166291	
103	HIG84	C	Higueruela	Spain	38,97	-1,43	KP166617	KP166984			
	HIG85	C	Higueruela	Spain	38,97	-1,43	KP166618	KP166985			
104	OMO58	C	Ossa de Montiel	Spain	39,00	-2,69	KP166684	KP167051			
	LEZ23	C	Lezuza	Spain	39,02	-2,38	KP166675	KP167042			
	LEZ24	C	Lezuza	Spain	39,02	-2,38	KP166676	KP167043			
105	LEZ15	C	Lezuza	Spain	39,03	-2,32	KP166673	KP167040			
	LEZ16	C	Lezuza	Spain	39,03	-2,32	KP166674	KP167041			
106	PDR05	C	Puebla de Don Rodrigo	Spain	39,08	-4,61	KP166685	KP167052			
107	DAI60	C	Parque Nacional Tablas de Daimiel	Spain	39,14	-3,69	KP166612	KP166979			
	DAI61	C	Parque Nacional Tablas de Daimiel	Spain	39,14	-3,69	KP166613	KP166980			
	IMS1558	C	Malagón	Spain	39,18	-3,91	KP166627	KP166994	KP166042-KP166043	KP166218-KP166219	
	IMS1559	C	Malagón	Spain	39,18	-3,91	KP166628	KP166995	KP165930-KP165931	KP166220-KP166221	
108	MAL01	C	Malagón	Spain	39,18	-3,91	KP166678	KP167045	KP166028-KP166029	KP166312-KP166313	
	MAL02	C	Malagón	Spain	39,18	-3,91	KP166679	KP167046			
109	IMS1578	C	Las Labores	Spain	39,29	-3,49	KP166629	KP166996	KP166044-KP166045	KP166222-KP166223	
	IMS1579	C	Las Labores	Spain	39,29	-3,49	KP166630	KP166997	KP165932-KP165933	KP166224-KP166225	
110	IMS1587	C	Pueblonuevo de Bullaque	Spain	39,31	-4,26	KP166631	KP166998	KP165934-	KP166226-	

									KP165935	KP166227	
	IMS1588	C	Pueblonuevo de Bullaque	Spain	39,31	-4,26	KP166632	KP166999	KP166046-KP166047		
	CAB01	C	Parque Nacional de Cabañeros	Spain	39,29	-4,33	KP166599	KP166966			
	CAB02	C	Parque Nacional de Cabañeros	Spain	39,29	-4,33	KP166600	KP166967			
111	IMS1538	C	Herencia	Spain	39,38	-3,30	KP166625	KP166992	KP165926-KP165927	KP166214-KP166215	
	IMS1539	C	Herencia	Spain	39,38	-3,30	KP166626	KP166993	KP165928-KP165929	KP166216-KP166217	
112	IMS1659	C	Urda	Spain	39,45	-3,81	KP166637	KP167004	KP166048-KP166049		
	IMS1660	C	Urda	Spain	39,45	-3,81	KP166638	KP167005	KP166050-KP166051	KP166230-KP166231	
113	IMS1533	C	El Toboso	Spain	39,49	-2,98	KP166623	KP166990	KP165924-KP165925	KP166212-KP166213	
	IMS1534	C	El Toboso	Spain	39,49	-2,98	KP166624	KP166991			
114	IMS1618	C	Marjaliza	Spain	39,51	-4,11	KP166633	KP167000			
	IMS1619	C	Marjaliza	Spain	39,51	-4,11	KP166634	KP167001			
	IMS1640	C	Marjaliza	Spain	39,52	-4,07	KP166635	KP167002	KP165936-KP165937	KP166228-KP166229	
	IMS1641	C	Marjaliza	Spain	39,52	-4,07	KP166636	KP167003	KP165938-KP165939		
115	IMS1976	C	Las Nogueras	Spain	39,59	-1,09	KP166655	KP167022	KP166058-KP166059	KP166256-KP166257	
	IMS1977	C	Las Nogueras	Spain	39,59	-1,09	KP166656	KP167023	KP166070-	KP166258-	

									KP166071	KP166259	
116	IMS1513	C	Villacañas	Spain	39,63	-3,36	KP166621	KP166988	KP166038-KP166039	KP166208-KP166209	
	IMS1514	C	Villacañas	Spain	39,63	-3,36	KP166622	KP166989	KP166040-KP166041	KP166210-KP166211	
117	IMS2786	C	Navahermosa	Spain	39,66	-4,42	KP166662	KP167029	KP165958-KP165959	KP166270-KP166271	
	IMS2787	C	Navahermosa	Spain	39,66	-4,42	KP166663	KP167030	KP165960-KP165961	KP166272-KP166273	
118	IMS2051	C	Alcublas	Spain	39,83	-0,66	KP166657	KP167024	KP166062-KP166063	KP166260-KP166261	
	IMS2052	C	Alcublas	Spain	39,83	-0,66	KP166658	KP167025	KP166064-KP166065	KP166262-KP166263	
119	PHS3	C	Cerro Pelado	Spain	39,86	-4,09	KP166686	KP167053	KP166092-KP166093		
	PHS4	C	Cerro Pelado	Spain	39,86	-4,09	KP166687	KP167054	KP166094-KP166095	KP166316-KP166317	
120	LTO02	C	La Toba	Spain	39,94	-1,70	KP166677	KP167044	KP165992-KP165993		
121	IMS3158	C	Camino del Sumidero, Los Palancares	Spain	40,02	-1,98	KP166664	KP167031	KP165968-KP165969	KP166274-KP166275	
	IMS3159	C	Camino del Sumidero, Los Palancares	Spain	40,02	-1,98	KP166665	KP167032	KP165970-KP165971	KP166276-KP166277	
122	IMS1751	C	Soto de Oreja, Ontígola	Spain	40,04	-3,51	KP166639	KP167006	KP166052-KP166053		

	IMS1752	C	Soto de Oreja, Ontígola	Spain	40,04	-3,51	KP166640	KP167007	KP165940-KP165941		
123	PP300	C	Valdepuercos	Spain	40,06	-3,30	KP166706	KP167073	KP166088-KP166089	KP166342-KP166343	
	PP301	C	Valdepuercos	Spain	40,06	-3,30	KP166707	KP167074	KP166090-KP166091	KP166344-KP166345	
124	PP01	C	Altos de Palomero, Ciempozuelos	Spain	40,13	-3,62	KP166689	KP167056			
125	IMS1756	C	Castillejos, Fuentidueña	Spain	40,14	-3,14	KP166641	KP167008	KP166054-KP166055	KP166232-KP166233	
	IMS1757	C	Castillejos, Fuentidueña	Spain	40,14	-3,14	KP166642	KP167009	KP165942-KP165943	KP166234-KP166235	
	IMS1781	C	Estremera	Spain	40,15	-3,12	KP166643	KP167010	KP166056-KP166057	KP166236-KP166237	
	IMS1782	C	Estremera	Spain	40,15	-3,12	KP166644	KP167011			
126	PP278	C	Valdemoro	Spain	40,18	-3,66	KP166704	KP167071	KP166084-KP166085	KP166338-KP166339	
	PP279	C	Valdemoro	Spain	40,18	-3,66	KP166705	KP167072	KP166086-KP166087	KP166340-KP166341	
127	PP142	C	Morata de Tajuña	Spain	40,24	-3,43	KP166694	KP167061	KP166080-KP166081	KP166326-KP166327	
	PP143	C	Morata de Tajuña	Spain	40,24	-3,43	KP166695	KP167062	KP166000-KP166001	KP166328-KP166329	
128	PP21	C	La Boyeriza, camino de Polvorines	Spain	40,26	-3,56	KP166698	KP167065	KP166006-KP166007	KP166330-KP166331	
	PP22	C	La Boyeriza, camino de Polvorines	Spain	40,26	-3,56	KP166699	KP167066	KP166096-		

									KP166097		
129	PP42	C	Carabaña	Spain	40,27	-3,25	KP166708	KP167075	KP166098-KP166099	KP166346-KP166347	
	PP43	C	Carabaña	Spain	40,27	-3,25	KP166709	KP167076	KP166014-KP166015	KP166348-KP166349	
130	IMS1511	C	Camino de Preresa (La Aldehuela) Getafe	Spain	40,30	-3,60	KP166619	KP166986	KP166034-KP166035	KP166204-KP166205	
	IMS1512	C	Camino de Preresa (La Aldehuela) Getafe	Spain	40,30	-3,60	KP166620	KP166987	KP166036-KP166037	KP166206-KP166207	
131	PP166	C	Arroyo de la Vega	Spain	40,32	-3,20	KP166696	KP167063	KP166002-KP166003		
	PP167	C	Arroyo de la Vega	Spain	40,32	-3,20	KP166697	KP167064	KP166004-KP166005		
132	PP102	C	Pozuelo del Rey	Spain	40,37	-3,32	KP166690	KP167057	KP166076-KP166077	KP166318-KP166319	
	PP103	C	Pozuelo del Rey	Spain	40,37	-3,32	KP166691	KP167058	KP166078-KP166079	KP166320-KP166321	
133	PP248	C	Pezuela del Rey	Spain	40,37	-3,18	KP166702	KP167069	KP166010-KP166011		
	PP249	C	Pezuela del Rey	Spain	40,37	-3,18	KP166703	KP167070	KP166012-KP166013	KP166336-KP166337	
134	PP62	C	La Yesera, Rivas Vaciamadrid	Spain	40,39	-3,52	KP166710	KP167077	KP166100-KP166101	KP166350-KP166351	
	PP63	C	La Yesera, Rivas Vaciamadrid	Spain	40,39	-3,52	KP166711	KP167078	KP166102-KP166103	KP166352-KP166353	

	PP82	C	La Guindalera, San Fernando de Henares	Spain	40,41	-3,50	KP166712	KP167078	KP166016-KP166017		
	PP83	C	La Guindalera, San Fernando de Henares	Spain	40,41	-3,50	KP166713	KP167080	KP166018-KP166019	KP166354-KP166355	
135	PP228	C	Las Cruces, Pezuela del Rey	Spain	40,42	-3,17	KP166700	KP167067	KP166082-KP166083	KP166332-KP166333	
	PP229	C	Las Cruces, Pezuela del Rey	Spain	40,42	-3,17	KP166701	KP167068	KP166008-KP166009	KP166334-KP166335	
136	IMS2116	C	Cedrillas	Spain	40,46	-0,86	KP166661	KP167028	KP165954-KP165955	KP166266-KP166267	
	IMS2117	-	Cedrillas	Spain	40,46	-0,86			KP165956-KP165957	KP166268-KP166269	
137	IMS2081	C	Ares del Maestre	Spain	40,46	-0,17	KP166659	KP167026			
	IMS2082	C	Ares del Maestre	Spain	40,46	-0,17	KP166660	KP167027	KP165952-KP165953	KP166264-KP166265	
138	PP122	C	Santorcaz a Los Santos de la Humosa	Spain	40,48	-3,24	KP166692	KP167059	KP165996-KP165997	KP166322-KP166323	
	PP123	C	Santorcaz a Los Santos de la Humosa	Spain	40,48	-3,24	KP166693	KP167060	KP165998-KP165999	KP166324-KP166325	
139	IMS3203	C	Revilla de Campos	Spain	42,01	-4,71	KP166666	KP167033	KP166066-KP166067	KP166278-KP166279	
	IMS3204	C	Revilla de Campos	Spain	42,01	-4,71	KP166667	KP167034	KP165972-KP165973	KP166280-KP166281	
140	IMS3918	C	Loma de los Perdigones	Spain	42,11	-1,39	KP166670	KP167037	KP165976-KP165977		

	IMS3919	C	Loma de los Perdigones	Spain	42,11	-1,39	KP166671	KP167038	KP166070-KP166071		
141	IMS3876	C	Arnedo, La Maja	Spain	42,29	-2,04	KP166668	KP167035	KP165974-KP165975		
	IMS3877	C	Arnedo, La Maja	Spain	42,29	-2,04	KP166669	KP167036	KP166068-KP166069		
142	BUR02	C	Páramo de Masa	Spain	42,66	-3,78	KP166598	KP166965	KP166026-KP166027	KP166298-KP166299	
143	Barna01	D	Castellet i la Gornal	Spain	41,25	1,59	KP166734	KP167101	KP166112-KP166113	KP166382-KP166383	Cyto-nuclear discordance (*β-fibint7*)
	Barna02	D	Castellet i la Gornal	Spain	41,25	1,59	KP166735	KP167102		KP166384-KP166385	Cyto-nuclear discordance (*PPP3CAint4*) (clades C+D)
144	GAR03	D	El Garraf	Spain	41,27	1,84	KP166743	KP167110			
	GAR01	D	El Garraf	Spain	41,27	1,84	KP166741	KP167108	KP165990-KP165991	KP166304-KP166305	Cyto-nuclear discordance (*PPP3CAint4*) (clades C+D)
	GAR02	D	El Garraf	Spain	41,27	1,84	KP166742	KP167109	KP166074-KP166075	KP166302-KP166303	
145	IMS2498	D	Prades	Spain	41,80	1,58	KP166747	KP167114	KP166120-KP166121	KP166376-KP166377	
	IMS2499	D	Prades	Spain	41,80	1,58	KP166748	KP167115		KP166378-KP166379	
146	BRU128	D	El Brull (Osona)	Spain	41,80	2,26	KP166738	KP167105	KP166072-KP166073	KP166294-KP166295	
	BRU06	D	El Brull (Osona)	Spain	41,80	2,26	KP166736	KP167103	KP165984-KP165985	KP166296-KP166297	

	BRU08	D	El Brull (Osona)	Spain	41,80	2,26	KP166737	KP167104			
147	RIV01	D	Riudarenes	Spain	41,83	2,72	KP166756	KP167123		KP166394-KP166395	
	RIV02	D	Riudarenes	Spain	41,83	2,72	KP166757	KP167124		KP166396-KP166397	
148	IMS2477	D	Suria	Spain	41,85	1,79	KP166745	KP167112	KP166104-KP166105		
	IMS2478	D	Suria	Spain	41,85	1,79	KP166746	KP167113	KP166106-KP166107	KP166374-KP166375	
149	SOS04	D	Solsona	Spain	42,10	1,65	KP166765	KP167132			
	SOS05	D	Solsona	Spain	42,10	1,65	KP166766	KP167133	KP166032-KP166033	KP166356-KP166357	
	SOS06	D	Solsona	Spain	42,10	1,65	KP166767	KP167134		KP166358-KP166359	
150	LLA01	D	Llança	Spain	42,37	3,16	KP166751	KP167118	KP166116-KP166117	KP166306-KP166307	Cyto-nuclear discordance (*β-fibint7*) (clades C+D)
	LLA02	D	Llança	Spain	42,37	3,16	KP166752	KP167119			
151	Pataris	D	Mare de Pataris	France	43,57	3,70	KP166755	KP167122	KP166118-KP166119	KP166392-KP166393	
	Devois	D	Mare de Devois	France	43,57	3,69	KP166740	KP167107	KP166114-KP166115	KP166388-KP166389	
152	SUE2310	D	Mare du Mas de Sueuilles	France	43,57	3,70	KP166768	KP167135			
	CAZ1920	D	Cazevieille	France	43,57	3,69	KP166739	KP167106		KP166386-KP166387	
153	MLT10271	D	St. Martin de Castries	France	43,78	3,47	KP166753	KP167120		KP166390-	

										KP166391	
154	SML1808	D	La Boissière	France	43,83	3,75	KP166764	KP167131			
	MSE2150	D	Mare de St-Etienne	France	43,81	3,78	KP166754	KP167121			
155	SMI10280	D	Saint-Michel	France	43,85	3,39	KP166763	KP167130		KP166400-KP166401	
156	SAV02	D	Savona	Italy	44,18	8,37	KP166758	KP167125			
	SAV04	D	Savona	Italy	44,18	8,37	KP166759	KP167126			
	SAV06	D	Savona	Italy	44,18	8,37	KP166760	KP167127			
157	SBC01	D	Saint-Bonnet-en-Champsaur	France	44,68	6,08	KP166761	KP167128		KP166398-KP166399	
	SBC02	D	Saint-Bonnet-en-Champsaur	France	44,68	6,08	KP166762	KP167129			
158	IMS4024	D	Libourne	France	44,91	-0,27	KP166749	KP167116	KP166122-KP166123		
	IMS4026	D	Libourne	France	44,91	-0,27	KP166750	KP167117	KP166108-KP166109		
159	HAV01	D	Estuaire de la Seine	France	49,46	0,21	KP166744	KP167111			
160	AMB01	D	Ambleteuse	France	50,80	1,62	KP166731	KP167098	KP166110-KP166111	KP166380-KP166381	
	AMB03	D	Ambleteuse	France	50,80	1,62	KP166732	KP167099			
	AMB04	D	Ambleteuse	France	50,80	1,62	KP166733	KP167100			
161	Cauc01		Rize	Turkey			KP166402	KP166769			
	Cauc02		Rize	Turkey			KP166403	KP166770			
162	IMS4649		Uzungol	Turkey			KP166404	KP166771			
	IMS4650		Uzungol	Turkey			KP166405	KP166772			
	IMS4651		Uzungol	Turkey			KP166406	KP166773			

	IMS4652		Uzungol	Turkey			KP166407	KP166774			
	IMS4653		Uzungol	Turkey			KP166408	KP166775			

Table 2. Polymorphism statistics for the mitochondrial and nuclear markers analyzed in this study. (n) number of sequences; (h) number of haplotypes; (S) number of segregating sites; (Hd) haplotype diversity; (π) nucleotide diversity; (θw) Watterson's (1975) mutation parameter Theta. * P<0.05; ** P<0.01; *** P<0.001.

Marker	**n**	**h**	**S**	**Hd**	**Π**	**Θw**	**Tajima's D**	**Fu's Fs**	**R^2**
mtDNA									
All	360	151	219	0.962 ± 0.005	0.02780 ± 0.00053	0.02270 ± 0.00466	0.44539	-27.587*	0.0940
Lineage A	77	42	54	0.950 ± 0.016	0.00372 ± 0.00022	0.00736 ± 0.00209	-1.65515	-29.493**	0.0473*
Lineage B	94	34	41	0.792 ± 0.043	0.00123 ± 0.00015	0.00537 ± 0.00153	-2.45213**	-38.589**	0.0244**
Lineage C	151	55	67	0.881 ± 0.024	0.00154 ± 0.00012	0.00803 ± 0.00203	-2.51337***	-74.408***	0.0178**
Lineage D	38	20	35	0.940 ± 0.021	0.00640 ± 0.00061	0.00558 ± 0.00185	0.40513	-2.345	0.1298
β-fibint7	278	40	45	0.869 ± 0.014	0.00940 ± 0.00040	0.00965 ± 0.00144	-0.19297	-5.910	0.0783
PPP3CAint4	278	23	25	0.709 ± 0.027	0.00745 ± 0.00039	0.01026 ± 0.00289	-0.88614	-5.044	0.0577

Table 3. Average number of pairwise sequence differences (p-uncorrected distance) within (on the diagonal) and between the four major mtDNA clades in *Pelodytes*. The outgroup *P. caucasicus* is included for reference.

Clade	A	B	C	D	*P. caucasicus*
A	0.0037				
B	0.0445	0.0012			
C	0.0334	0.0408	0.0015		
D	0.0377	0.0444	0.0348	0.0064	
P. caucasicus	0.1574	0.1625	0.1683	0.1618	0.002

Table 4. SpedeSTEM results (multiple AIC calculations, similar results are recovered with the single AIC calculation, data not shown). K=number of clades; -lnL=negative logarithm of the likelihood function; AIC: Akaike information criterion; delta: difference in AIC score.

k	-lnL	AIC	delta
2	-28537.5314	57079.0628	1983.0597
3	-28547.5068	57101.0135	2005.0105
4	-27544.0015	55096.0030	0.000000

Figure1

Click here to download high resolution image

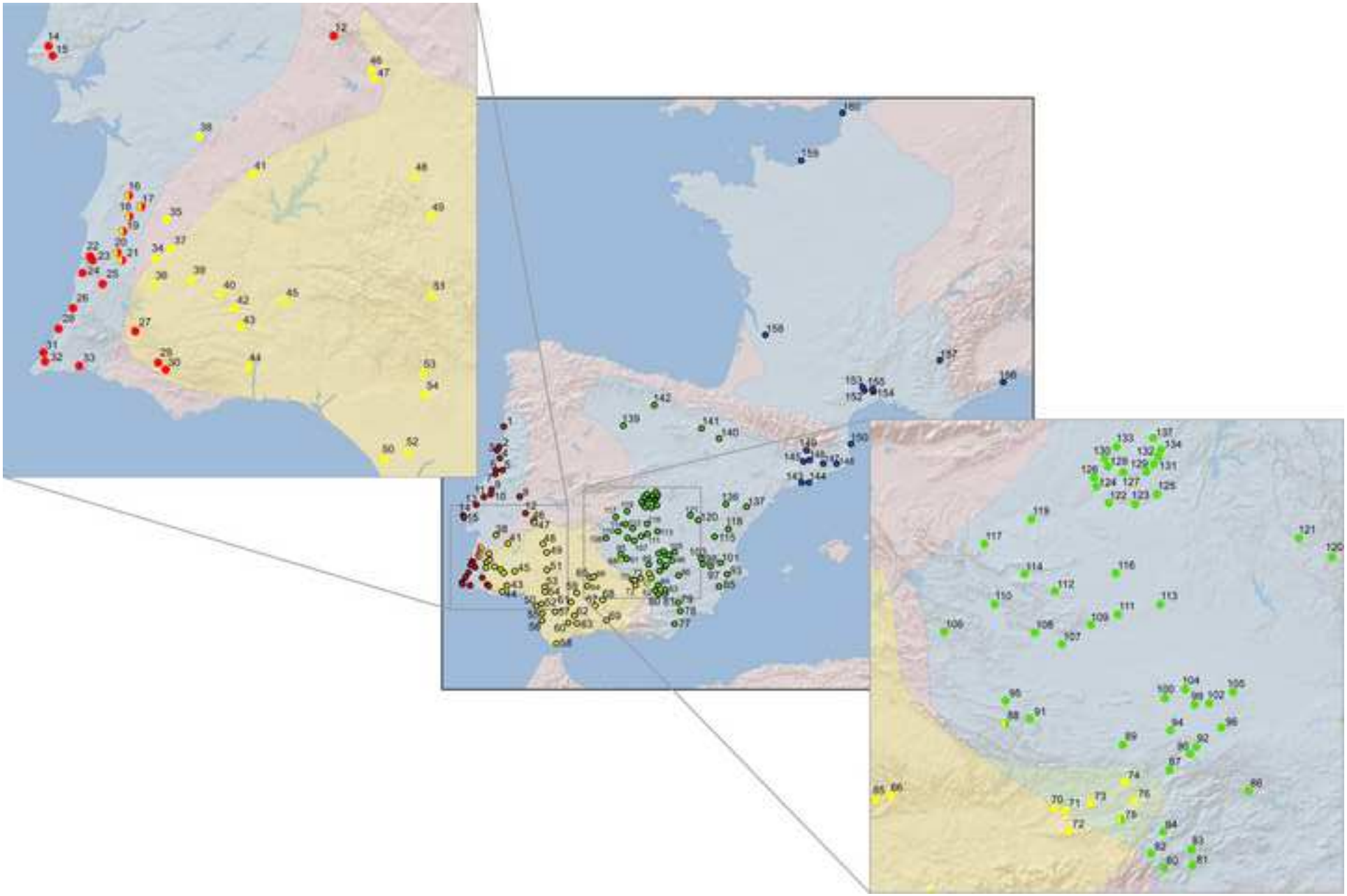

Figure2

Click here to download high resolution image

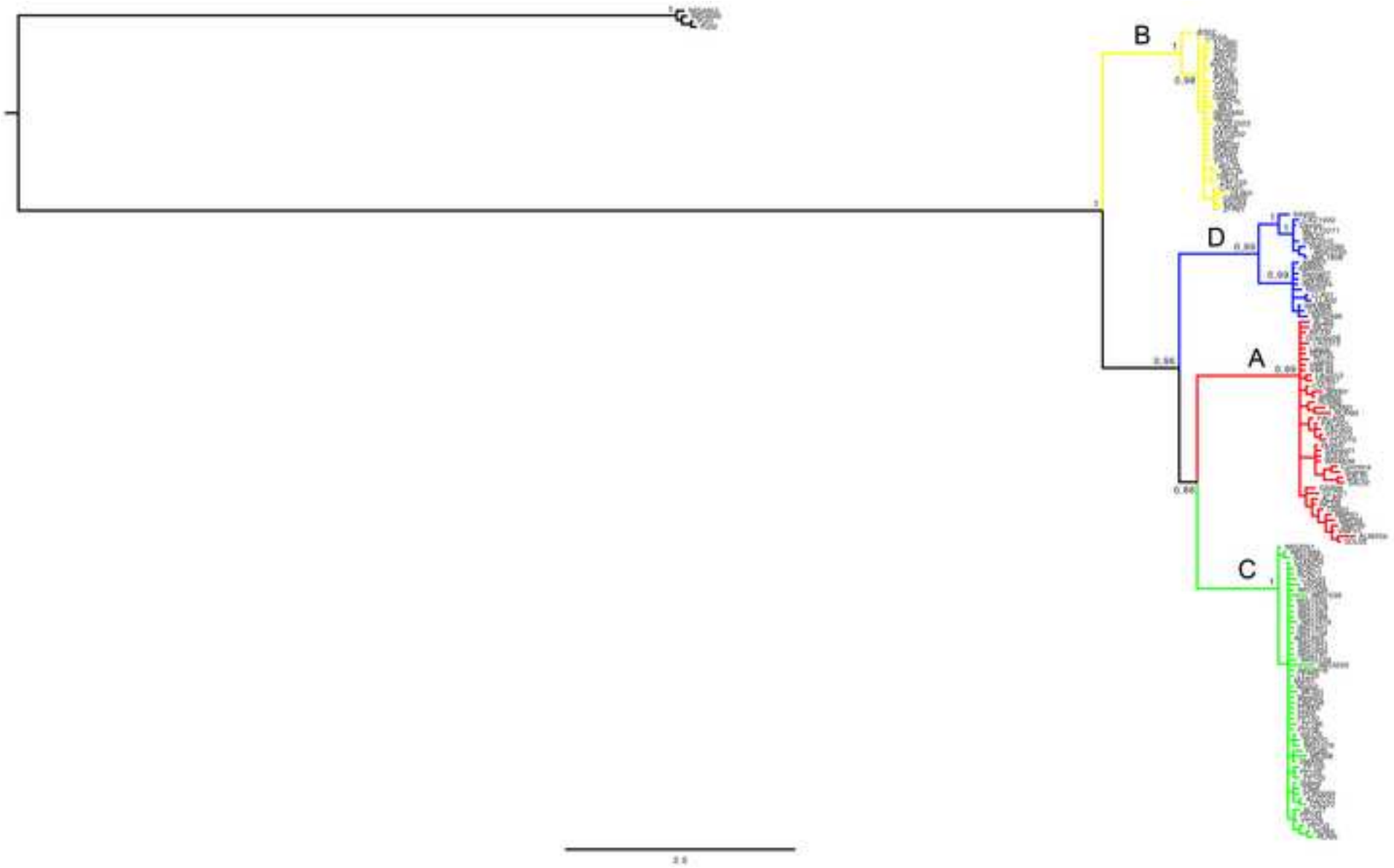

Figure3

Click here to download high resolution image

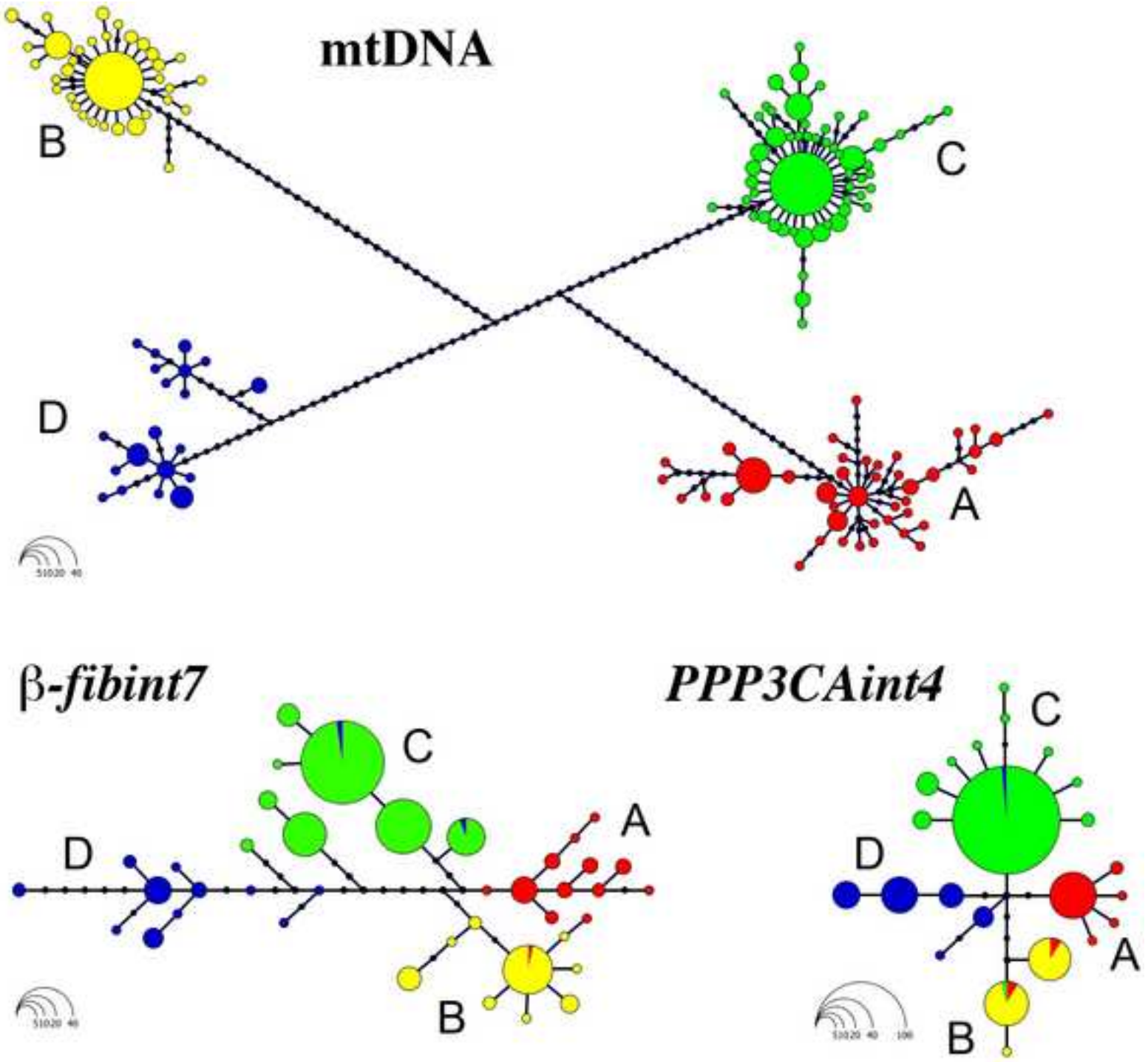

Figure4

Click here to download high resolution image

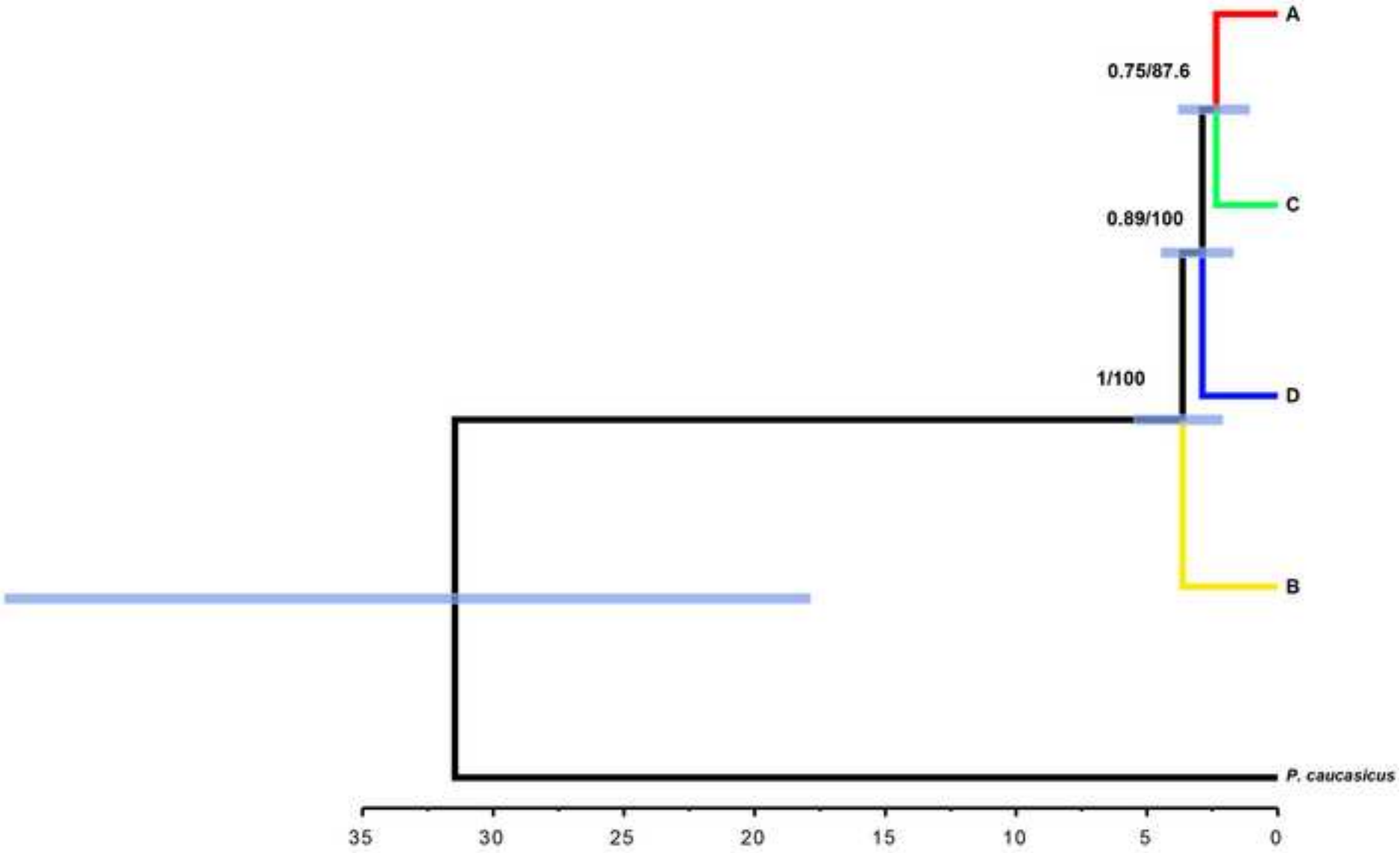

Supplementary Figure S1

Click here to download Supplementary Material: FigS1_rev.jpg